Journal of Materials Chemistry A

REVIEW

View Article Online
View Journal | View Issue

Cite this: J. Mater. Chem. A, 2019, 7, 21577

Nano-engineering and micromolecular science of polysilsesquioxane materials and their emerging applications

Numan Ahmed,[a] Hong Fan,*[a] Philippe Dubois,[b] Xianwei Zhang,[a] Shah Fahad,[a] Tariq Aziz[a] and Jintao Wan[c]

Received 2nd May 2019
Accepted 12th August 2019

DOI: 10.1039/c9ta04575a

rsc.li/materials-a

Polysilsesquioxanes $(RSiO_{1.5})_n$ are organic–inorganic hybrid materials that have an array of properties and synergistic features and are considered to be robust materials in the family of siliceous compounds. Their careful tailoring at the nano and micro scale has been investigated worldwide, as their architecture dictates the final properties. Non-porous nano and micro organosilica hybrid particles that have been designed using careful optimization of the effective parameters, for example the amount of monomer, reaction time, concentration of the catalyst, temperature, and stirring speed, are detailed in this article. Different sized particles comprising bridged, ladder-like, cage shape and other geometries modified by organically functionalized reagents are discussed. This review presents a summary of the recently reported nano and micro-sized polysilsesquioxanes with different functional materials and their geometries, describing their preparation methods and further applications in science and technology, especially those reported in the last half decade.

1 Introduction

Controlling the design of silsesquioxanes through self-assembly is one of the most exciting areas of research in polymer science and technology. The specific term silsesquioxane is the combination of (sil–) owing to the main atom silicone, (–sesquiox–) that bonds to 1.5 oxygen atoms in each part and (–ane) owing to the hydrocarbon group, which is the alkane. Each silsesquioxane molecule has an inorganic rigid core that is extended in three dimensions and it is the smallest stable silica particle that exists. The combination of self-assembly routes with the sol–gel process is perhaps the most attractive and promising route for obtaining sophisticated silsesquioxane hybrids ranging from the nanometer to the micrometer size, which exhibit a variety of physical–chemical characteristics with

[a]State Key Laboratory of Chemical Engineering, College of Chemical and Biological Engineering, Zhejiang University, Zheda Road no. 38, Xihu District, Hangzhou 310027, China. E-mail: hfan@zju.edu.cn

[b]Center of Innovation and Research in Materials and Polymers (CIRMAP), University of Mons UMONS, Place du Parc 20, Mons B-700, Belgium

[c]Shaanxi Normal University, School of Materials Science and Engineering, Xi'an 710119, China

Numan Ahmed Attari is a Ph.D candidate at the College of Chemical and Biochemical Engineering of Zhejiang University. His research interests are focused on the synthesis, optimization and modification of nano and micro sized functional silicone materials for advanced applications in science and technology.

Hong Fan received his Ph.D in chemical engineering at Zhejiang University in 1989. He has been a professor at the College of Chemical and Biochemical Engineering of Zhejiang University since 2008. His research interests are focused on nano and micro sized silicone product engineering, fluoro and silicone containing fine chemicals, adhesives and materials, design and preparation of novel thermoset polymers and high performance composites.

additional functionalities and radical new properties.[1,2] Controlling the final molecular structure, size and function of these systems is often a delicate process that requires vigilant customization and an understanding of the synthesis details to avoid possible side reactions such as gelation, crosslinking, and cyclization.[3] However, this variation in size is responsible for the wide range of modifications in the basic skeleton of the Si–O bond. This aspect affords a polysilsesquioxane network with the desired morphology, size, porosity (pore volume and diameter) and physical properties.[4] Until now, a large number of functional groups have been modified with this organic–inorganic based hybrid material owing to its adaptable nature, and a variety of different potential applications that benefit mankind have emerged, from small household items to large industrial scale objects. Polysilsesquioxanes (PSQs) are inorganic–organic hybrid silica particles that have a three-dimensional network with the general formula $(RSiO_{1.5})_n$, in which R = H, alkyl, aryl, halogens, and so forth, which are then called hydridosilsesquioxanes,[5,6] alkylsilsesquioxanes, arylsilsesquioxanes, and halosilsesquioxanes, respectively. Silsesquioxanes can assume various structural forms and serve different applications, owing to the combination of the siloxane (Si–O–Si) bonded networks with the organic constituents, as shown in Fig. 1. The three main classes of this family are generally reported to be ladder-like, random branched polymers, and spherical shape silsesquioxanes.[7–13] Silsesquioxanes exhibit brilliant features in terms of their mechanical properties, a good thermal stability, chemical resistance, extraordinary oxygen plasma etching resistance, ultralow dielectric constant, and even their biocompatibility.[4,14–17] These molecules can be readily functionalized to modulate their properties, for example, by adjusting the interfacial properties or creating reactive sites to increase their solubility and compatibility with organic matrices. The types of organic periphery affects the accumulation and characteristic phase transition of the molecules.[18–22] Nano-sized silsesquioxane particles are usually prepared in acidic medium with the help of ethanol as the main solvent. After that, the condensation process is carried out using a high concentration of ammonia with a high stirring speed of 600–900 rpm.[23] This method results in a wide range of

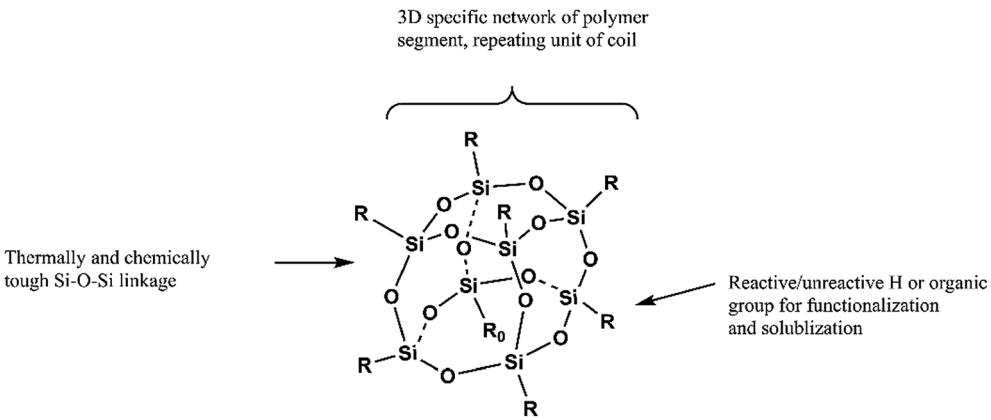

Fig. 1 Essential features of the silsesquioxane unit structure.

Philippe Dubois received his Ph.D in Science (Chemistry) in 1991 and undertook a postdoc in Chemical Engineering. At present he is the rector-president at University of Mons-UMONS, Mons (Belgium), scientific director & President at Materia Nova Research Center, director at Center of Innovation and Research in Materials & Polymers CIRMAP. His research interests are focused on organic chemistry, organometallic catalysis, macromolecular chemistry, engineering of polymeric and nano composite materials, and the key-role of "green" chemistry in nanotechnology and materials science.

Jintao Wan received his Ph.D in chemical engineering at Zhejiang University in 2010. After his postdoctoral work at Zhejiang University, he worked as a research scientist at IMDEA (Institute of Materials Research and Advanced Studies Madrid, Spain). In 2017 he joined the School of Materials Science and Engineering faculty at Shaanxi Normal University. His research interests are focused on silicone based polymer product engineering, epoxy resin and its composite materials.

nanoparticles from 600 to 2 nm.[24–26] On the other hand, micro-sized silsesquioxane particles have been prepared in either acidic or alkaline media with the help of water as a solvent and finally condensed by a moderate concentration of an alkaline base or ammonium hydroxide with a low stirring rate from 100–400 rpm that produces a size range from 1 to 10 μm. All of the resulting nano and microparticles and their final geometries are produced by using simple organosilane(s) X–SiY_3 (in which X and Y represent the different functional groups and Y usually hydrolyzes during the reaction) precursor(s). When the organosilane(s) are hydrolyzed into a solvent using the sol–gel process they form different geometrical shapes according to their mechanism and exhibit different applications dependent on their functional groups (see Fig. 2).[23,27,28] Recently, some researchers have modified the silsesquioxane nanoparticles in different ways with CeO_2, ethyl, phenyl, polypropylene, methacrylate and mercaptopropyl[29–34] for use as catalyst carriers, treatment materials for pollution control, UV screening agents, picking emulsifiers, bioimaging applications, drug and gene delivery, photodynamic therapy applications, superhydrophobic materials, and for improving the nano tribomechanical properties, as well as inorganic nanofillers.[4,9,17,33,35,36] These inorganic nanofillers have been used as promising nanomaterials to reinforce polymers. The most favorable nanofillers include layered silicates (2D), single and multi-walled nanotubes (1D), carbon nanofibers (1D), and polyhedral oligomeric silsesquioxane nanostructures (0D). On the other hand, silsesquioxane microparticles have been modified with chloropropyl moieties to support the catalytic properties in the epoxidation of alkenes, salicylic acid for UV protection, cetyltrimethylammonium for making aerogels, and allyl alcohols for making polyurethane based composites.[37–39] Other modified PSQs have been used for cargo delivery, as a storage source of electrochemical energy, gas adsorption, microreactors and so on.[40] On the whole, PSQs have been successfully incorporated into various polymers such as styrenes, polyesters, acrylates, polyimides, polyolefins, and polyurethanes.[41–43]

The present review emphasizes the intense efforts from recent years devoted to the design of organosilica particles with different size ranges, along with geometrical shapes promoted by the concomitant occurrence of hydrolysis/condensation reactions and self-directed assembly/self-organization routes, through the judicious choice of synthesis conditions and the rational design of the precursor (modification with different functional groups and the number of repeating units). Polyhedral oligomeric silsesquioxanes (POSS) are silsesquioxane polyhedra nano-scale particles. As the frontier between these two materials is very narrow and could be prepared by using the same starting material trimethoxyorganosilanes some examples of this class will also be highlighted. As many reviewers have discussed the different applications and synthesis aspects of silsesquioxanes materials over the years, little attention has been paid to reviewing the size of the silsesquioxane particles. This review endeavors to provide the following benefits to readers: (i) a reader-friendly overview of the broad field of modified silsesquioxane materials on the basis of the size; (ii) provide a route to find the research gaps and trends in the field of controlled size silsesquioxanes; and (iii) discuss the relevant applications of these modified materials in science and technology. All of this practical and practicable information has

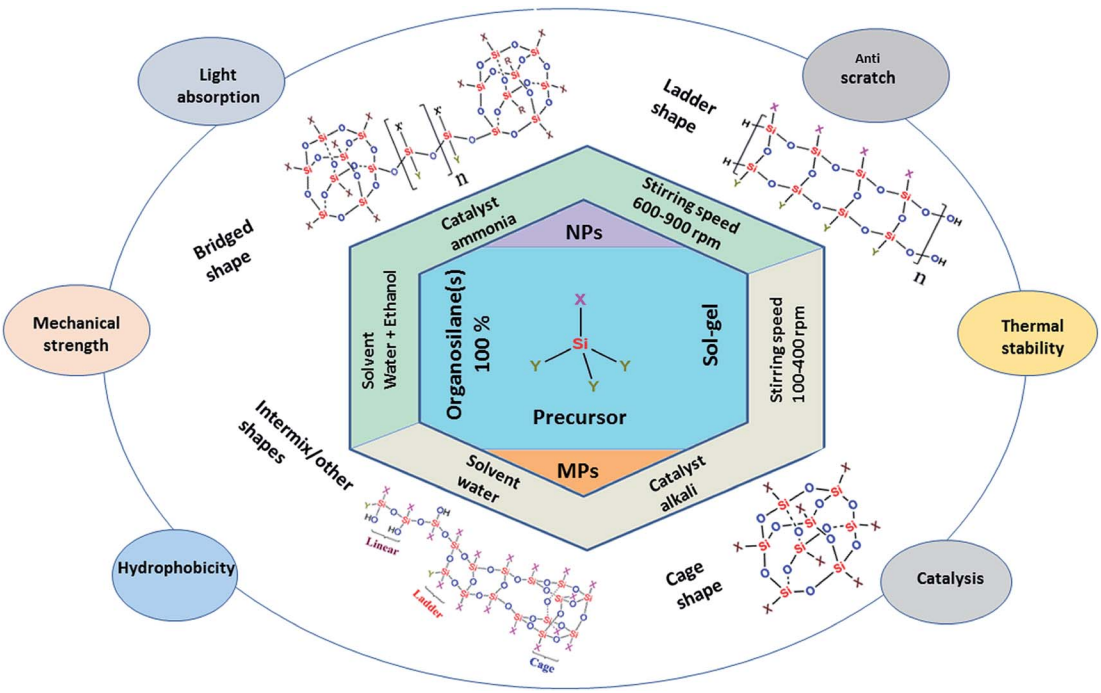

Fig. 2 Schematic overview of the preparation of nano and micro-sized silsesquioxanes, their size controlling factors, different resulting shapes and common properties.

been summarized using recent scenarios for researchers in the relevant fields.

1.1 Mechanism of PSQs growth

When the silane precursor (methyltrimethoxysilane (MTMS) or methyltriethoxysilane (MTES)) is hydrolyzed in water with an acid as a catalyst then silanols and its dimers are formed. These species then react with OH^- produced by the base catalyst to generate the silica anions, which go on to conduct nucleophilic attacks on the silanols and dimers generating the initial Si–O–Si backbones,[44–46] as shown in Fig. 3. The effect of the stirring speed on the size of the silsesquioxane spheres is illustrated in Table 1. Although the pH, concentration of the monomer, amount of surfactant and temperature also affect the size, the stirring speed is the most pronounced factor among them.

When the stirring speed decreases from 900 to 100 rpm, the resultant silsesquioxane spherical particles retain their regular morphologies, but their particle size increases from 229 to 1215 nm while the average particle size distribution becomes narrower.[47,48] It can be deduced that by increasing the stirring speed, which actually increases the shear force, a good dispersion of the silane precursor is favored. The faster the stirring speed, the more the interface contact between the nucleation site and the hydrolytic monomer become disturbed, which hinders the stable growth of the silsesquioxane spheres and increases the size distribution of the silsesquioxane particles.

Table 1 The influence of the stirring speed on the size of the PSQs

Sample number	Stirring speed (rpm)	Average diameter (nm)
1	900	229 (±60)
2	700	477 (±50)
3	500	859 (±30)
4	300	1008 (±28)
5	100	1215 (±15)

Eventually, the resultant oligomers are shaped to spherical polysilsesquioxanes and their size can be controlled by managing the stirring speed. In terms of the concentration of the monomer, the saturation and supersaturation of the monomer in the solvent affects the homogeneous nucleation process in the solution. During the reaction, the surfactant molecules overlay the surface of the silsesquioxane particles which prevent their agglomeration and gives them a good colloidal stability.[49]

1.2 General preparation scheme for different PSQs

To date, many PSQs have been modified with numerous functional moieties to give fascinating properties.[18] Herein, Fig. 4 provides us with an overview to understand the basis of many modifications for the reader.

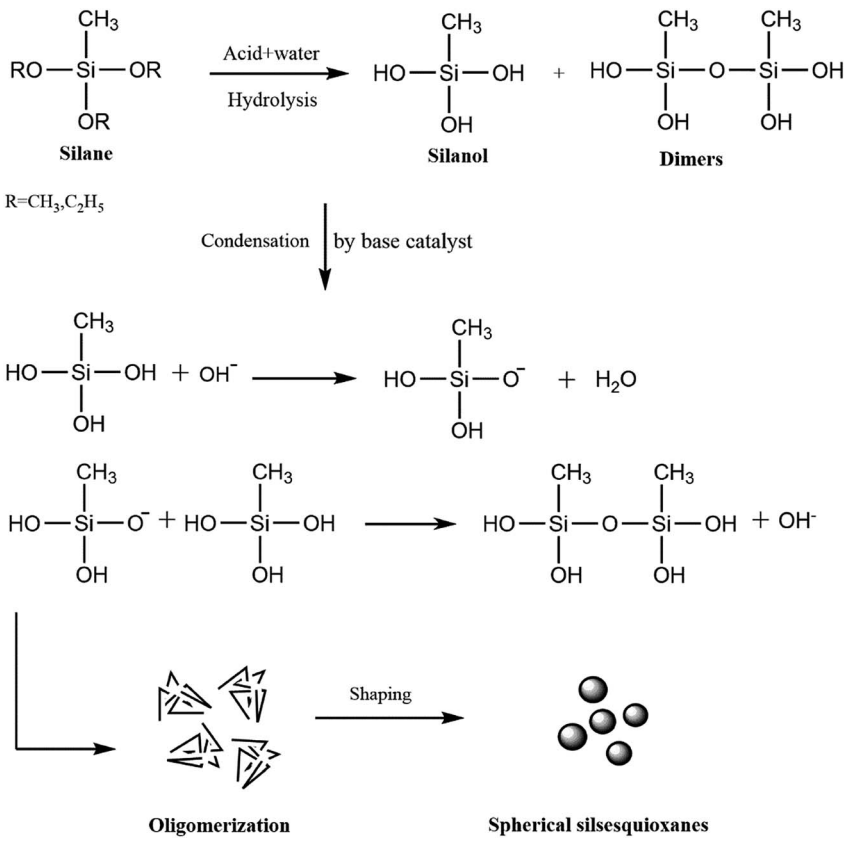

Fig. 3 Mechanism of the growth of the PSQs.

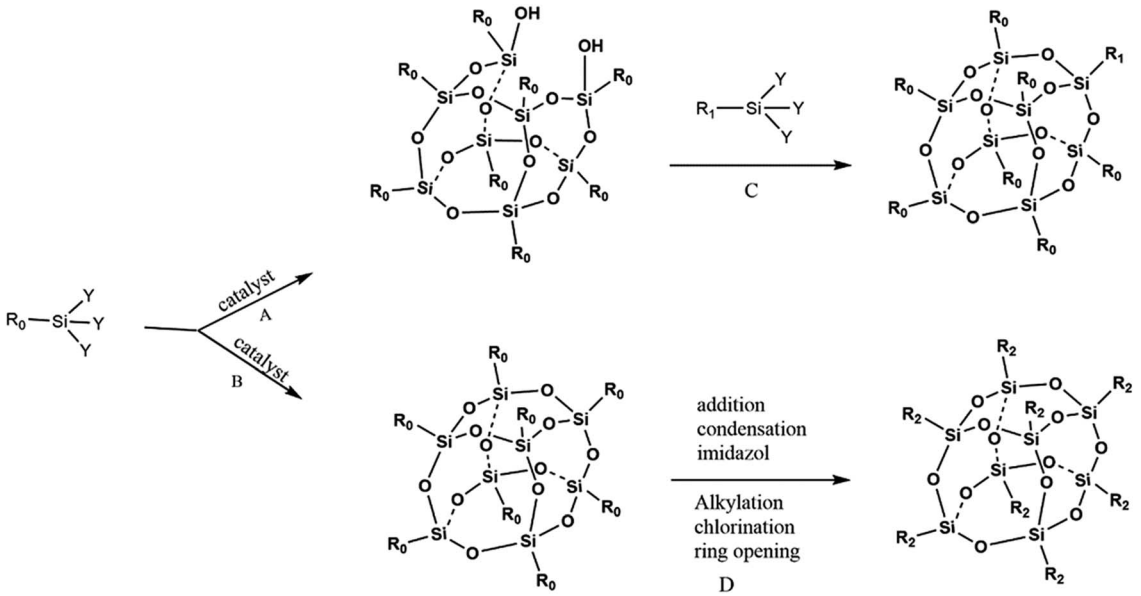

Fig. 4 General preparation scheme for different silsesquioxanes.

Type (A) reactions (Fig. 4) are incomplete condensation reactions, which leads to an incomplete silsesquioxane structure according to the synthetic conditions. In particular, different trisilanols with one missing edge can be easily obtained with highly sterically hindered substituents such as cyclohexyl and phenyl.[50,51]

Type (B) reactions (Fig. 4) consist of the direct and complete condensation of trichlorosilanes or trimethoxy/ethoxy/propoxysilanes owing to the starting R_0SiY precursors. These precursors lead to the formation of POSS $(R_0SiO_{1.5})_n$ derivatives which have even number 'n' values of 4–12. Although R_0 groups can be alkyd, amide, imidazolium, thiol, hydrogen, methyl, ethyl, *n*-pentyl, *n*-hexyl, cyclohexyl, phenyl, and some other substituted epoxy groups[52–54] most of the R_0 substituents are small groups as the steric hindrance of large organic groups means it is difficult to obtain a complete condensation.

Type (C) reactions are the corner capping reactions of those POSS structures that came into being by an incomplete condensation reaction. As shown in Fig. 4, the incomplete cage can react with the functional R_1SiY_3 to gain a complete POSS moiety. This method can allow the specific control of the final POSS structure. The construction provides a way to generate a multi-functional group and metal bearing POSS, in which the multi-functional host groups or transition metal elements are introduced into the POSS network.[55–57]

Type (D) reactions are basically the modification of the complete POSS cages obtained from one of the three above mentioned methods through a second reaction step by the incorporation of R_2 groups depending on their chemical structures (Fig. 4). For example, POSS modified by phenyl results in octaphenyl. This is considered to be a robust, thermally stable, and high-temperature polymer. Owing to its compact structure, it is highly insoluble and non-reactive, which results in poor compatibility with different polymer matrices when used as a filler. Whereas, when further modified by a polar species, for example sulfonic acid, nitrate, amine and so forth, this octaphenyl POSS becomes soluble and compatible with other polymers.[58,59]

2 Nano-sized polysilsesquioxanes

The nano-sized PSQs in the range of 2–600 nm can be prepared by careful optimization of the amount of solvent, the concentration of the monomer and catalyst, the amount of surfactant, the duration of the reaction, and the stirring speed. Therefore, an increase in the amount of solvent and catalyst, the concentration of the monomer, and the duration of the reaction increase the final size. While the increase in the stirring speed and the concentration of the surfactant decrease the final size of the silsesquioxanes, the effect of the stirring speed and the concentration of the monomer are especially intense in comparison to the other parameters. Therefore, in general with a reduced saturation of the monomer concentration 0.3–0.2 mol L^{-1}, a short span of time 24–2 h, a small amount of base catalyst 0.6–0.1 mol L^{-1}, a large amount of solvent 2.5–10 mol, a high concentration of surfactant 3.0–10.0 g and a fast stirring rate 600–900 rpm,[23,47,60–64] the nucleation process becomes slower, resulting in nano-sized silsesquioxanes.[49]

Thus, by following this streamlined mechanistic behavior, bridged, ladder-like, pendant, cage shape and intermixed

silsesquioxane structures have been made by researchers.[65–68] Along with size control, the different silsesquioxane structures were generated by using their respective precursors and other reaction conditions. In general, these are shown in Fig. 5 to help the reader understand the relationship of size control with the respective geometries.

2.1 Bridged silsesquioxanes

The silsesquioxanes that are connected to each other ($O_{1.5}Si–R–SiO_{1.5}$) by a functional moiety that links them together are considered to be bridged silsesquioxanes (BS).[69–71] Croissant *et al.*, prepared a novel two-photon photosensitizer with the help of a sol–gel process with or without gold NPs, which led to bridged silsesquioxanes nanoparticles (BSNPs) and gold-doped BSNPs by using a two-photon excited photodynamic therapy (TPE-PDT) technique (Fig. 6).[31]

For the same TPE-PDT technique, Chiara *et al.*, prepared another type of bridged silsesquioxane nanoparticles by using phthalocyanine (PHT) and porphyrin (POR) as a precursor. For this POR and PHT were first reacted with alkoxysilane by using a click coupling cycloaddition reaction in the presence of an azide–alkyne copper catalyst at 100 °C for 15 min under microwave irradiation. Afterwards, using a surfactant and a basic solution, porphyrin-based and phthalocyanine-based bridged silsesquioxanes were prepared in a hot mixture of ethanol and dimethyl sulfoxide (DMSO) solvents under stirring at 750 rpm for 2 h. The high amount of surfactant reduced the probability of the agglomeration of the particles and resulted in monodisperse NPs. Similar types of metal and non-metal containing bridged silsesquioxanes have been developed using a unique method for the formation of an E–O–Si bond (E = Si, Ge and B) by using scandium(III) trifluoromethanesulfonate, which includes the *O*-metalation of silanols with 2-methylallylgermananes or 2-methylallylsilanes. The successful use of scandium(III) triflate in the *O*-silylation of the bridged POSS silanols using 2-methylallylsilanes was also reported. Inspired by these results, this methodology was extended for the preparation of germanium-functionalized silsesquioxanes, as well as POSS derivatives, containing Ge atoms incorporated into the POSS backbone (Fig. 7).

Therefore, Ge-functionalized bridged POSS compounds were successfully obtained which consisted of two nanometer sized

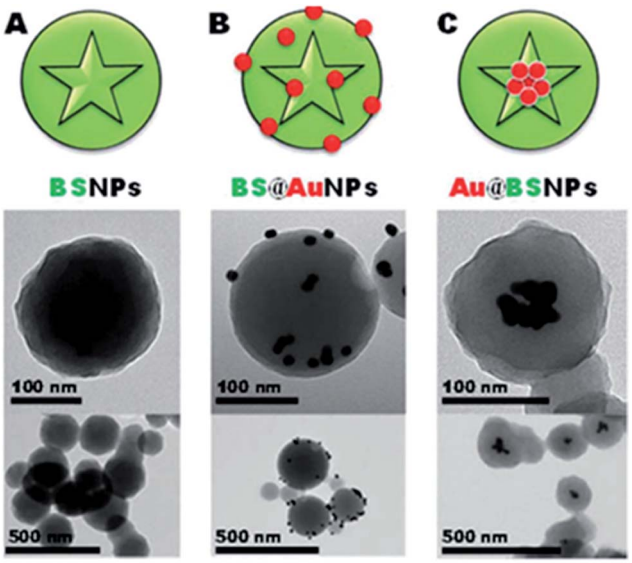

Fig. 6 Representation of BSNPs, BS@AuNPs, and Au@BSNPs along with their TEM images (a–c). Adapted with permission from ref. 31. Copyright 2016, Royal Society of Chemistry.

POSS molecules that were connected together by an organo-germanium functionality that had never been made before.[72] By following a similar theme, another bridged/necklace-shaped POSS with dimethylsiloxane (DMS) copolymers with "alternating modulated chain" arrangements was prepared by Katsuta *et al.*, they claimed that the three different kinds of chain arrangements of polymers can also be produced along with "constant chain" and "random chain" type polymers. The main structure of the POSS-DMS polymer can be customized, using the substituents, average molecular weight, molecular weight distribution, and chain length arrangement. These results indicated the importance of the primary structure in relation to the design of bridged shape polymers and the effect on the physical properties.[73]

2.2 Ladder-like silsesquioxanes

The ladder-like structure of polysilsesquioxane (PSQ) is considered to be one of the most regular and soluble structures of this family. These compounds usually have the following

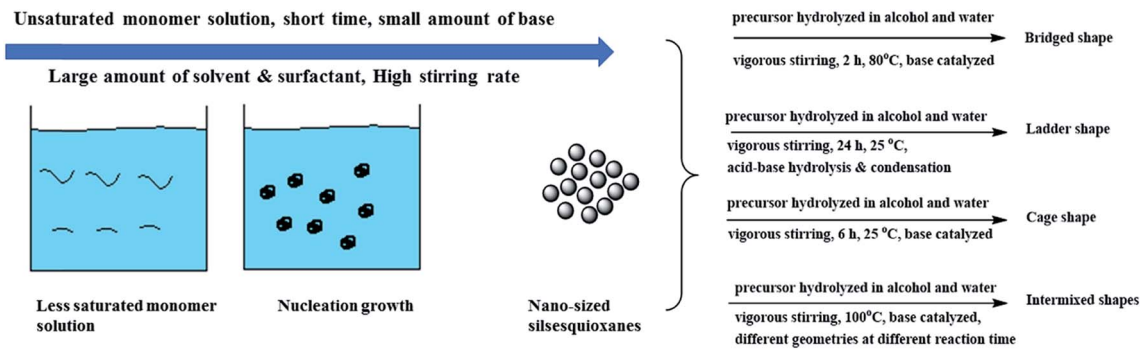

Fig. 5 A concept diagram of different nano-sized silsesquioxanes and their size control.

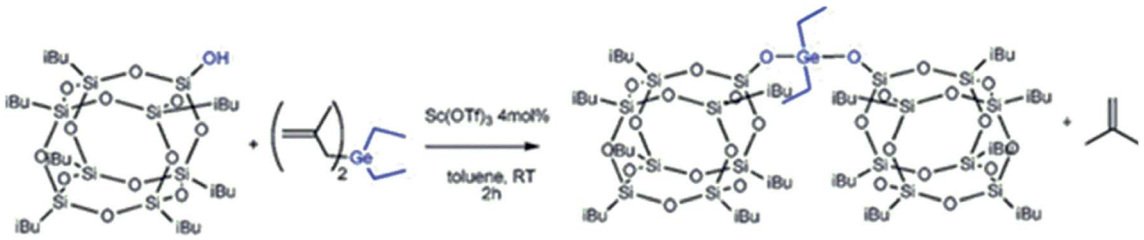

Fig. 7 Synthesis of Ge-functionalized bridged POSS derivative. Adapted with permission from ref. 72. Copyright 2017, American Chemical Society.

characteristics: (i) one-dimensional structures with relatively small molecular widths that do not form branch chains; (ii) a large peak at −67.25 ppm and a small peak at −58.41 ppm which can be observed in the ^{29}Si NMR spectra (Fig. 8), which is the only evidence of a small number of silanol groups; (iii) it is soluble; therefore, it does not tend to form a PSQ with a three-dimensional (random) network structure; and (iv) it has a relatively high molecular weight, which indicates that it does not form an oligomeric silsesquioxane.

Some ladder polymethylsilsesquioxane (PMSQ) nanoparticles with average particle sizes of 15–20 nm were prepared by Baatti *et al.*, by using MTMS through a hydrolysis and condensation process.[74] At first, moisture free MTMS was hydrolyzed using HCl under vigorous stirring followed by condensation with NaOH.[65,75–78] The mechanism is illustrated in Fig. 9, in which the acidic H^+ attacks the water molecule and splits it into H^+ and OH^-.

The OH^- further promotes the nucleophilic addition which thereby improves the rate of hydrolysis. Fig. 9 shows that the hydrolysis is a rapid protonation equilibrium of MTMS leaving the HO–CH_3 group. Condensation always occurs in acidic media which usually has a pH value of less than 2. In addition, the formation of cyclic compounds under acidic conditions is a common feature of the polymerization of the Si–OR group. Therefore, although the Raman measurements cannot identify

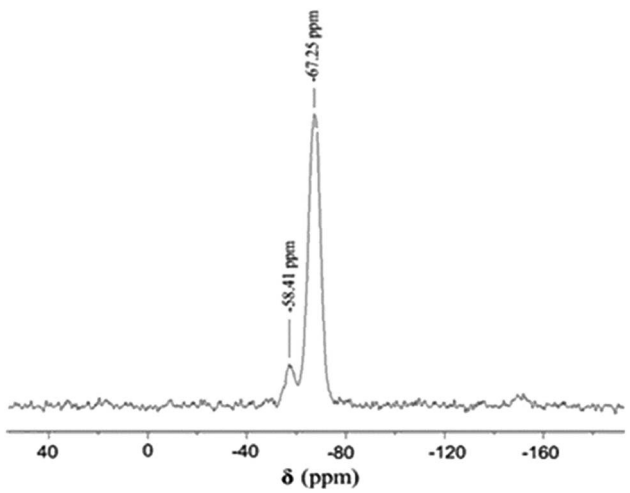

Fig. 8 ^{29}Si NMR spectra of ladder silsesquioxane. Adapted with permission from ref. 74. Copyright 2017, Elsevier.

such ring structures, it is suggested that the silanol groups hydrolyzed from MTMS can react with each other to form a ring structure of four silicon atoms connected by a siloxane bond (Si–O–Si) with an OH group at the end of the cycle resulting in the formation of a precursor followed by the formation of the final ladder PMSQ polymer. The development of the gel formation and the ladder PMSQ structure occurs in basic media. Actually, some positive charges on the silicon atoms increase with the increase of the connectivity, which contributes to the nucleophilic addition of the Si–OH functions on the silicon atoms. The hydrolysis mechanism consists of a series of equilibria in which an increase in the water concentration slightly moves the hydrolysis rate, which makes the reaction irreversible. Therefore, according to the H_2O stoichiometric content of the MTMS hydrolysis reaction, the molar ratio of the methoxy group and water in MTMS used in this study was about 3.[74] Harada *et al.*, prepared a soluble ladder-like PSQ by using concentrated HCl as a catalyst in the hydrolytic polycondensation reaction of 2(diethoxyphosphoryl)ethyltriethoxysilane (PETES) with phosphonic acid side-chain groups, PSQ-PO_3H_2. By using concentrated HCl, the ethoxyphosphoryl group in PETES is changed into a phosphonic acid group by a simple hydrolysis reaction. The phosphonic acid group is ionic and its incorporation is necessary for the preparation of soluble PSQ with a regular structure. A soluble ladder-like (rod-like) PSQ with a phosphonate side chain group (PSQ-PO_3HK) was prepared by treating PSQ-PO_3H_2 with potassium hydroxide aqueous solution (KOH) resulting in a hexagonal stacking structure in the solid state. This PSQ-PO_3H_2 has high proton conductivity and excellent thermal stability, and is a potential proton conductive electrolyte for fuel cells that operates in the 100–200 °C temperature range.[79] Hwang *et al.* synthesized a series of ladder shape polysilsesquioxanes (LPSQs) with a fixed methacryloxpropyl (MA)/R molar ratio (6 : 4) containing the UV curable MA group and different organic functional (R) groups (naphthyl, phenyl, propyl, hexyl, and cyclohexyl), as hard coating materials. Changing the R groups in these LPSQs enabled the researchers to recognize the effects of the different chemical structures of the UV-cured LPSQs films on their related mechanical properties, for example cyclization, cyclic *versus* acyclic (hexyl *vs.* cyclohexyl), the aliphatic number of carbons (propyl *vs.* hexyl), the extent of aromaticity (phenyl *vs.* naphthyl) and aliphatic *versus* aromatic (cyclohexyl *vs.* phenyl).[80] Another four types of self-healing ladder-structured polysilsesquioxanes named poly(*n*-

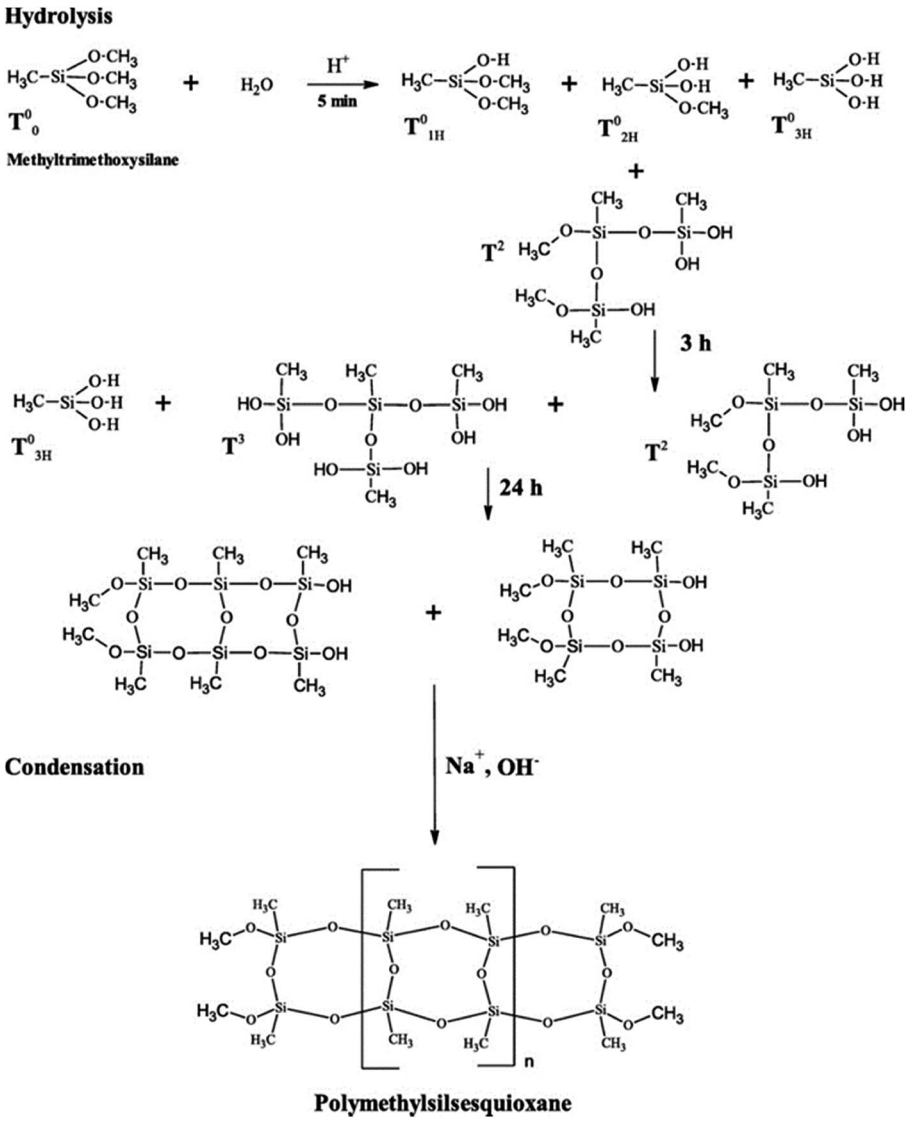

Fig. 9 Reaction scheme for ladder PMSQ. Adapted with permission from ref. 74. Copyright 2017, Elsevier.

propylpyrrole-*co*-cyclohexenylethyl)silsesquioxane LPCSQ55, LPrPCSQ244, LHPCSQ244, and LDPCSQ244 were successfully prepared and their Diels–Alder (DA) and retro-Diels–Alder (rDA) self-healing properties were analyzed through scratch tests. A series of copolymers with different alkyl lengths were synthesized and the effects of chain mobility were investigated. For LPCSQ55, *N*-(3-trimethoxysilylpropyl)pyrrole (2.29 g, 0.04 mol) and 2-(3-cyclohexenyl)ethyltrimethoxysilane (2.30 g, 0.04 mol) were used. Although LPrPCSQ244, LHPCSQ244, and LDPCSQ244 were prepared by using propyltrimethoxysilane, hexyltrimethoxysilane, and dodecyltrimethoxysilane as additional materials along with the aforementioned chemicals, respectively, it was observed that with an increase of the length of an alkyl chain, the mobility of the chain increased, while the DA reaction of the LPCSQ copolymer with a long chain was slow. This was due to the large distance between the chains.[81] Using sodium cyclosiloxanate as a precursor, another kind of soluble silsesquioxanes with a regular ladder structure containing phenyl (LPSQ-ph) was synthesized by *in situ* polycondensation of $[PhSi(O)OH]_4$. Based on the molecular weight analysis, the composition changes of the oligomers in the reaction mixture were revealed, which indicated that a large number of cyclic compounds formed at the beginning of the reaction which were converted into linear oligomers. The type of cyclic LPSQ-ph and the redistribution of the reaction product in the presence of a base were also observed using the oligomer obtained *via* the step-by-step coupling polymerization. The stability of the ladder silsesquioxane produced by the polycondensation method of cyclic tetrasiloxanetetraols (PCT) has a different thermal stability compared to the ladder silsesquioxane obtained by a step-wise coupling polymerization (SCP). In this process, a hard black glass was formed, and the LPSQ-Ph prepared by SCP was transformed into a fragile ceramic.[82] In addition, using a similar sol–gel method, a novel ladder-like structured methacrylate siloxane hybrid material (LMSH) with 3-(trimethoxysilyl)propyl methacrylate (MPTMS) using water as a solvent was

prepared. Under the inert dry N_2 gas flow the mixture was first hydrolyzed for 1 h at 65 °C, and then condensed using the base for 3 h at 80 °C. The production of this material took 4 h without any additional solvent and the resulting LMSH exhibited a high optical transparency (90.6% at 550 nm) and a high thermal stability (T5 wt% decomposition > 400 °C) compared to commercial cage-structured PSQs and random-structured siloxane hybrid materials. The good mechanical properties and the excellent heat resistance of the LMSH originates from the regularity of the siloxane structure, the highest density of the siloxane-methacrylate co-networks, and its molecular level hybridization.[83]

2.3 Cage shape silsesquioxanes

The cage-like silsesquioxanes are a large division of the polycyclic siloxanes compounds. Generally cage-shaped silsesquioxanes are well-defined siloxanes having a robust core of 1.5 nm diameter.[66] Swapna *et al.*, prepared the cage-shaped POSS based PVA poly(vinyl alcohol) membrane by using a solution casting method.[66] At first PVA with modified POSS (m-POSS) were mixed together with a different weight percentage of POSS and the membranes were prepared by slowly transferring the POSS into the PVA solution by stirring it for 4 h followed by ultrasonication and drying in oven at 40 °C for 48 h. Fig. 10c shows the PVA/m-POSS membrane in which the POSS particles can be observed in the surface of the polymer matrix. The nano-sized POSS fillers are easy to agglomerate, but this phenomenon cannot be observed for POSS particles at a lower percentage in the PVA matrix. This membrane showed a good mechanical stability and pervaporation performance for the isolation of water from the isopropanol mixture.

Some cage-shape silsesquioxanes contain organic functional moieties while some contain a metal atom as an essential part which shows outstanding properties in catalysis, these are called metallasilsesquioxanes. In this category four types of this kind of unusual nano-sized cage-like complexes were prepared (see Fig. 10a and b) by using Cu(II)-methylsilsesquioxanes and varying the nature of the solvents and/or N ligands, namely, nona-$[(MeSiO_{1.5})_{18}\text{-}(CuO)_9]$ **1**, hexa-$[(MeSiO_{1.5})_{10}(HO_{0.5})_2(\text{-}CuO)_6(C_{12}H_8N_2)2\text{-}(MeSiO_{1.5})_{10}(HO_{0.5})_{1.33}(CH_3COO_{0.5})_{0.67}(CuO)_6(C_{12}H_8N_2)_2]$ **2**, $[(MeSiO_{1.5})_{10}(CuO)_6(MeO_{0.5})_2(C_{10}H_8N_2)_2]$ **3**, and trinuclear $[(MeSiO_{1.5})_8(CuO)_3(C_{10}H_8N_2)_2]$ **4**.

Compounds **1** and **4** were the first cage-like metallasilsesquioxanes (CLMSs), containing nine and three copper(II) ions, respectively. Furthermore, cage complex 1 was the first ever example of a nonanuclear metallasilsesquioxane. Owing to the specific size of its cavity having an internal diameter greater than 8 Å, this special structure appears to have potential as a host compound. In these silsesquioxanes, compound 1 catalyzed the homogeneous phase oxidation of either alkanes to alkyl hydroperoxides or alcohols to ketones. This molecular structure was obtained from very simple starting reagents, and this highlights the important prospects for this new synthetic pathway (Fig. 11a).

In further research the first example of an unusual pentanuclear cage-like Ni(II)-based silsesquioxane cage-like metallasilsesquioxane (CLMS) was designed. The novel hexanuclear $[(PhSiO_{1.5})_{12}(NiO)_6(H_2O)(DMSO)_9]$ **1** was obtained by adding DMSO solvent and the $[(PhSiO_{1.5})_{10}(NiO)_5(DMF)_7]$ **2** nickel(II)-based silsesquioxanes were obtained by the exchange reaction of sodium phenylsiloxane phenylsiloxanolate $[PhSi(O)ONa]_n$ and $NiCl_2\cdot 6NH_3$ by using dimethylformamide (DMF) (Fig. 11b). The aforementioned discussion proves that the role of the solvents in the synthesis process is very important for the nucleation of the final compounds. Therefore, a possible method for the assembly of pentanuclear complexes, that is the coordination of DMF molecules was proposed for these cage silsesquioxanes. These two compounds were studied using topological analysis and an X-ray diffraction method. The results of the magnetic properties showed that in both cases, the existence of magnetization was caused by the spin glass-like behavior, which was instigated by the spin disturbance in each multinuclear complex and the dipole interaction between the CLMS molecules.[84] In the same sense Rungthip *et al.*, synthesized cage like POSS particles for the detection of Hg^{2+} by functionalizing the particles with rhodamine hydrazide receptors (T10Rh). This POSS sensor was synthesized and its sensing behavior for metal ions was studied using ultraviolet/visible and fluorescence spectroscopy. The sensor underwent color and

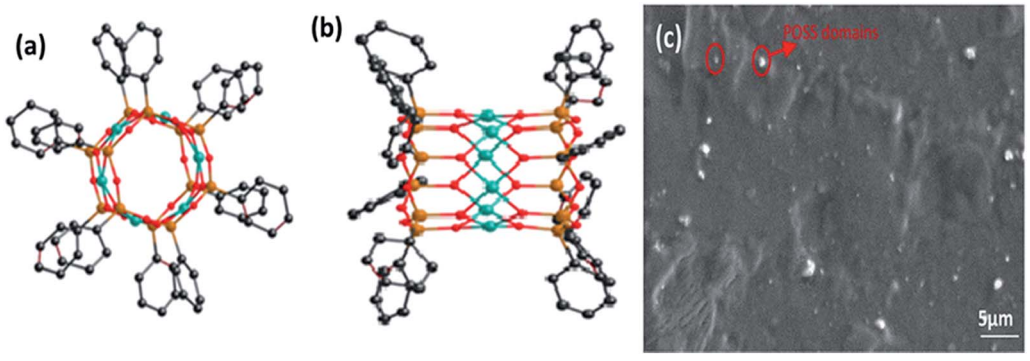

Fig. 10 (a) and (b) General view of the cage-like metallasilsesquioxane. Adapted with permission from ref. 56, copyright 2017, American Chemical Society. (c) PVA CTAB-modified octa-TMA-POSS glutaraldehyde (POCPG3). Adapted with permission from ref. 66 copyright 2019, Springer Nature.

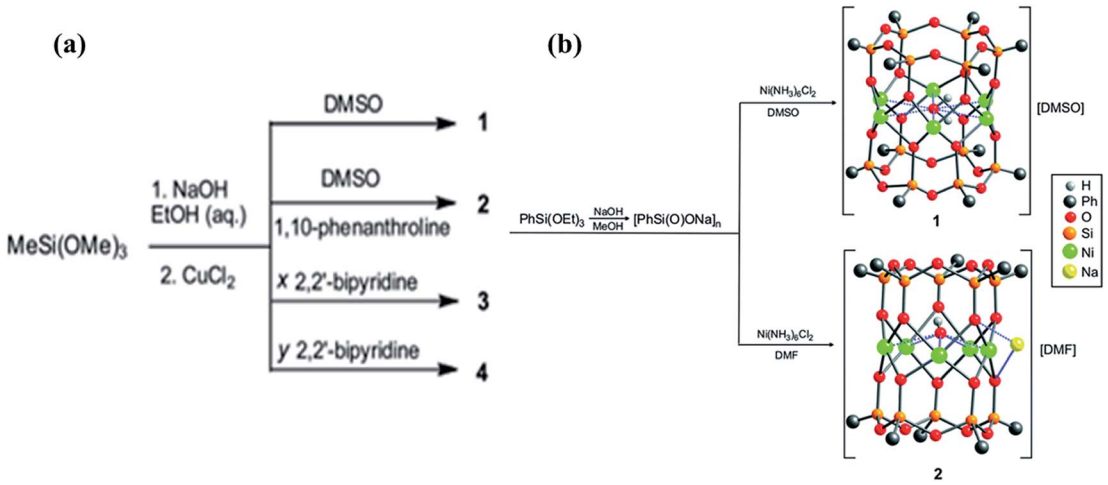

Fig. 11 (a) A general scheme of synthesis for the CLMSs **1–4**. Adapted with permission from ref. 56 copyright 2017, American Chemical Society. (b) Schematic representation of the synthetic strategy employed for designing the hexanuclear $[(PhSiO_{1.5})_{12}(NiO)_6(H_2O)(DMSO)9]$ **1** and the pentanuclear $[(PhSiO_{1.5})_{10}(NiO)_5(DMF)_7]$ **2** phenylsilsesquioxanes. Adapted with permission from ref. 84 copyright 2016, Wiley.

fluorescence changes upon Hg^{2+} detection, and also exhibited significant color changes in aqueous solutions (from colorless to pink-red in color). This material proved to be highly soluble in an ethanol aqueous solution, having a high selectivity and sensitivity for mercury(II) ion detection even at very low detection limits (3.14×10^{-9} M or 0.63 ppb), which is below the maximum allowable level of inorganic Hg metal (2 ppb) in drinking water. The analysis revealed that the selective binding leads to the transition of the structure of T10Rh from the spirolactam (non-fluorescent) form to the non-cyclic (fluorescent) form,[85] as shown by the ON–OFF fluorescence signal from Hg^{2+} binding. It was compared with some alkali (Li^+, Na^+, K^+), alkaline earth (Mg^{2+},Ba^{2+}, Ca^{2+}) and other (Cu^{2+}, Ag^+, Pb^{2+}, Al^{3+}, Cd^{2+}, Ni^{2+}, Fe^{2+}, CO^{2+}, Mn^{2+}, Zn^{2+}) metal ions with detection limits of 0.63 ppb. The concentration used was lower than the drinking water concentration permissible by the U.S. Environmental Protection Agency (U.S. EPA) and the World Health Organization (WHO).[86] A cage-type oligomeric silsesquioxane (POSS) room temperature ionic liquid (IL) with two side chain groups was successfully prepared by the hydrolysis–condensation reaction of two organo trialkoxysilane mixtures. One silane contained 1-methyl-3-[3-(triethoxysilyl)propyl]imidazolium chloride (MTICl) and the other contained a quaternary ammonium group, trimethyl[3(triethoxysilyl)propyl]ammonium chloride (TTACl). Together, these two ionic liquids (ILs) were denoted as Amim-Cage-SQ-IL. A methanol and water mixture was used as a solvent for TTACl (resulting in a POSS called Am-Cage-SQ-IL) and only water was used for MTICl (resulting in a POSS called Im-Cage-SQ) along with the super acid bis(trifluoromethanesulfonyl)imide HNTf2. The differential scanning calorimetry (DSC) curves for Amim-Cage-SQ-IL showed a baseline deviation at −8 °C owing to the T_g and their visible flow temperature was about 30 °C, for example ionic liquids. The flow temperature was significantly lower than that of Im-Cage-SQ-IL (*ca.* 100 °C) and Am-Cage-SQ (*ca.* 155 °C) prepared using MTICl and TTACl, respectively. On the basis of these facts Amim-Cage-SQ-IL is an amorphous compound. In addition, the pyrolysis temperatures of the SQ frame in the ILs were extremely high (414, 420 and 428 °C for Td3, Td5, and Td10 respectively).[52] In addition, the waterborne epoxy and alkyd resin were prepared and the effect of the epoxy resin (ER) along with the cage shaped 3-glycidyloxypropyl-POSS (G-POSS) content, on their properties, was examined by Huo *et al.* The alkyd resin was synthesized using castor oil, trimethylolpropane, and 1 wt% *N*,*N*′-dimethyl benzylamine heated to 145 °C with slow stirring for about 90 min. Afterward, benzoic acid along with isophthalic acid was added and heated to 225 °C to make the acid value of the solution lower than that of 10 mg of KOH per g. 3-Glycidyloxypropyl containing POSS ER was prepared with a mixture of 10% tetramethylammonium hydroxide (TMAH), 3-glycidyloxypropyl-trimethoxysilane (GTMS) and isopropyl alcohols in aqueous solution. Finally, transparent viscous liquids with an 82% yield and an epoxy value of 0.50 mol/100 g were obtained which showed a high impact strength, and good electrical and insulating properties.[54]

2.4 Unspecified geometrical silsesquioxanes

Many researchers prepared various valuable materials by the modification of nano-sized PSQs of unspecified or intermixed geometry. This section presents a brief summary of such materials.

2.4.1 Intermixed geometrical silsesquioxanes. By using an *in situ* water production (ISWP) sol–gel strategy, D'Arienzo *et al.*, proposed a comparatively easy method for preparing adjustable ladder shape or cage shape thiol functionalized silsesquioxanes nano-building blocks (SH-NBBs) with an average hydrodynamic diameter of 2 nm (Fig. 12). Therefore, these materials could be appropriate candidates for the preparation of nanocomposites with specific properties.

To this end, a simple and fast solution mixing technique was used to add a low concentration thiol functionalized silsesquioxane nano-building block (SH-NBB) with a different

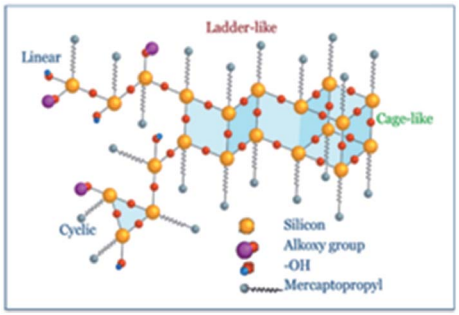

Fig. 12 Molecular architectures of the SH-NBBs. Adapted with permission from ref. 3 copyright 2018, Elsevier.

molecular structure in 1,4-polybutadiene (PB). The results showed that even very low, for example 1 and 3 wt% SH-NBBS loading can significantly reduce the mobility of the polymer chains and improve their mechanical properties, depending on the molecular structure of the fillers.[3]

2.4.2 Silsesquioxane aerogels. Silsesquioxane aerogels are very low-density nanoporous solids with exceptional properties, for example a high surface area and porosity, a reduced dielectric constant and thermal conductivity, and good optical transparency. Owing to these special characteristics, silsesquioxane aerogels have received widespread attention in the past few years. Typically, these silsesquioxane aerogels are prepared from organo trialkoxysilane as a starting substrate using the sol–gel method with the help of a two-step acid–base catalysis prior to draining the liquid from the wet gel by ambient pressure drying or a supercritical drying method. Similarly, PMSQ aerogels with an adjustable core size (10–40 nm) obtained by changing the ammonia concentration have also been reported. These aerogels were prepared by polycondensation of MTMS through hydrolysis in aqueous solution and macrophase separation was prevented by a surfactant. The saturation of the surfactant into the reaction mixture is also a reason for their fine nanosize.[87] Furthermore, a similar sol–gel technique was implemented to synthesize a superhydrophobic PMSQ aerogel with a porous network using MTMS reactants and cetyltrimethylammonium bromide (CTAB) surfactants. These CTAB-modified PMSQ aerogels were prepared with small CTAB/MTMS (C/M) molar ratios of 0.001, 0.002 and 0.004. When the pristine PMSQ aerogels were compared with the modified one, the precise surface area and pore size of the CTAB modified PMSQ aerogels was reduced, because the CTAB surfactant was adsorbed as a template on the pore surface of the aerogels, resulting in a reduced pore size. In addition, a CTAB surfactant was also used as a structural directing agent to adhere onto the surface of the PMSQ aerogels, to stabilize its skeleton and enhance its structural strength. The results showed that CTAB modified PMSQ aerogels possess solvent resistance in *n*-hexane and ethanol.[38]

2.4.3 Catalysis related silsesquioxanes. This section includes those nano-sized functional silsesquioxanes that can either act as a catalyst themselves or those that are generated after catalytical reactions. Herein, Kaźmierczak and colleagues have developed a unique catalytic pathway for the formation of Si–O–Si bonds in the coupling reaction of silanols with 2-methylallylsilanes catalyzed by scandium(III) trifluoromethanesulfonate. Here, they reported that this method has been successfully extended for the functionalization of silsesquioxane. This method proved to be a unique catalytic procedure for the corner-capping reaction to prepare a series of functionalized silsesquioxanes as shown in Fig. 13.

This unique method provides silsesquioxanes derivatives which have a good efficiency, high yield, and chemoselectivity that cannot be achieved using conventional methods.[88] The hydrosilylation of the CuC bond has also been investigated by another group using Karsdet's catalyst. This method proved to be an effective way to synthesize 1,2-(*E*)-disubstituted and 1,1,2-(*E*)-trisubstituted ethylene with silsesquioxane. Compared with the other procedures mentioned in the literature,[89,90] this method did not require special preparation of the catalyst, reagents, or purification of the inert gases. In addition, the actual reaction time was recorded for the first time, to determine the progress of hydrosilylation owing to the influence of the alkyne structure these parameters were determined using *in situ* Fourier transform infrared spectroscopy (FTIR), ^{1}H NMR, and FTIR spectroscopies. It was found that in a high concentration solution, the formation rate of the hydrogenation products of the triple bonds at the end and inside the alkynes was much faster. It is worth emphasizing that among all of the published literature, this is the first ever example of the hydrosilylation of the internal alkynes. As a result, the 1,1,2-(*E*)-trisubstituted ethenes with a monofunctional silsesquioxane moiety were formed. Along with the stereo defined products, double bonds also have other functions, such as 4-pinacol esters, 4-bromophenyl silyl or germyl groups, which allow them to be used for further chemical conversions, such as dehalogenation and demethylation (Si, B, Ge) and they have a widespread presence in organic synthesis methods such as the Suzuki–Miyazaki, Sonogahira, Heck and Hills coupling reactions. These nano building blocks can be used to prepare highly conjugated, completely soluble molecular or macromolecular systems with improved thermal, mechanical and photoelectric properties.[91] Another outstanding performance of Karsdet's catalyst, for the synthesis and design of a monoene substituted silsesquioxane library with a robust Si–O–Si architecture along with a functional part with different chain lengths (from vinyl to dec-9-ene) and five inert groups (Et, iBu, iOc, Cy, ph), was studied. The effective steps of synthesis were based on condensation, a corner-capped reaction, and the hydrosilylation process using the respective chlorosilanes, which are not all available on a commercial scale. As a result, they successfully prepared 40 compounds, more than half of which had not been described before. The solubility, crystallization and melting behavior, thermal stability, ductility and change in the glass transition point of these materials were analyzed. Their thermal analysis results showed a strong structure-thermal performance relationship. The synthesis conditions, adjustable reactivity, and accessibility of the functional groups (caused by different steric hindrances) were also investigated.[92] Using the same scenario for the catalyst based synthesis of

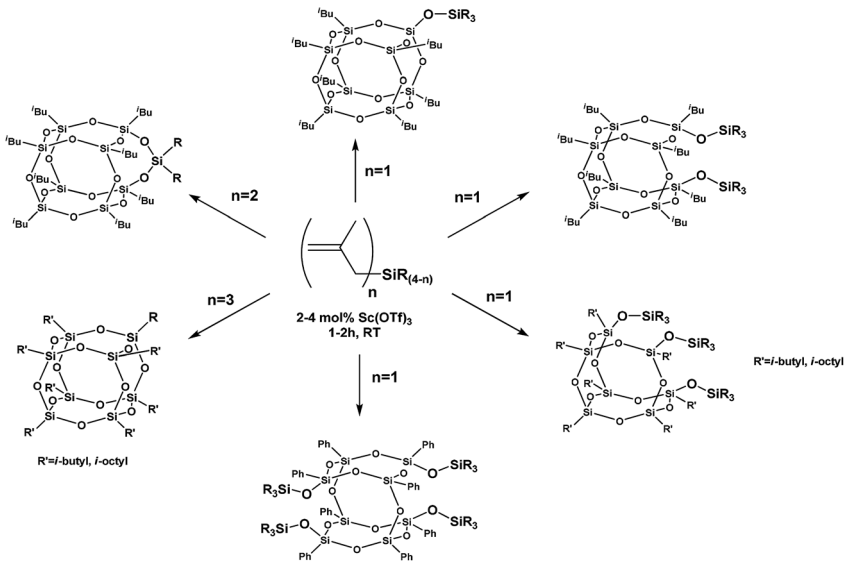

Fig. 13 Sc(OTf)3-catalyzed *O*-silylation of POSS silanols by 2-methylallylsilanes. Adapted with permission from ref. 88 copyright 2017, American Chemical Society.

functional silsesquioxane materials, a unique catalytic scheme was devised for the synthesis of a Si–O–E bond (E = Si, B, Ge), that was also applicable for many silsesquioxanes. In this case, the commercial polymer Nafion (sulfonated tetrafluoroethylene) was successfully proved to be a highly selective and efficient multiphase catalyst for the *O*-metallization of silanol, POSS silanol, germasiloxanes, borasiloxanes, and other siloxanes. The most amazing feature was that the activity of Nafion remained the same even after 10 catalytic steps, without reduction of the selectivity and yield. It was also used to precede different reactions of the silsesquioxanes derivatives, under optimized conditions, without producing harmful corrosive by-products.[93] On the other hand, an amazing effort allowed the successful preparation of a novel porous near infrared photoluminescent POSS-based material without a catalyst. A simple reaction was performed for the thermal hydrosilylation and polymerization of vinyl-POSS with hydrogen-terminated silicon nanocrystals (ncSi:H). For this, vinyl-POSS was added to the ncSi:H in the presence of decane as a solvent with careful removal of moisture and dissolvable oxygen under vacuum. By using the Schlenk technique, this mixture was then treated with dry argon and brown precipitates were finally obtained. Different analytical techniques confirmed the integrity of these POSS cages and their structural features remained the same within these nanocomposites.[94,95]

2.4.4 Silsesquioxane based membranes. Membranes are thin-layered films used for the permeability of different substances, selective solvent separation, and reclamation from liquids and gases. To make the membranes thermally and mechanically more stable and to improve the separation performance, silsesquioxane nanoparticles were used as fillers. The performance of POSS nanoparticles as a filler for a nanocomposite membrane for the purpose of separation was reviewed by Chen and Dumee. The silsesquioxane based nanocomposite membranes were used for vapor transportation, small molecule or ion rejection, and liquid separation driven by solvent separation, pressure, gas separation, desalination, and proton exchange membranes. In actual fact, the silsesquioxane particles acted as an interfacial modifier and tuned the spacing between the matrix and the nanoparticle support which resulted in a better separation ability. Another advantage of these types of membranes was that the selectivity of the system can be enhanced by adding the reactive functionalities on the corner of the POSS particles to adjust the surface charge.[20,96,97]

2.4.5 Silsesquioxane based metal–organic frameworks. Metal–organic frameworks (MOFs) usually contain metal ions or clusters that coordinate with organic ligands. Coordination bonds between the organic ligands and the transition metal have been commonly used in metal–organic coordination polymers and extended networks. However, the configuration of this extensively organized architecture is not so simple. These POSS with eight functional groups can be used as a three-dimensional and multi-functional ligand for the preparation of MOFs. Modification at every silicone corner can efficiently increase the number of metal cations doped into the mixtures. Usually, these MOFs have different shapes, but their morphological change (spheres to nano-plates and rings to rods) are all related to spectral changes, which indicate that the mixed complexes may be good candidates for functional substances with sensing abilities.[55] Yoon *et al.,* fabricated POSS particles with a metal–organic framework (MOF) with nodes of Zn ions and an azobenzene containing dicarboxylic acid. The resulting particles were then used for the preparation of highly hydrophobic liquid marbles (LMs). It was found that upon exposure to acidic vapors, the MOFs could not retain their original shape which revealed that these LMs have a good potential for the detection of acidic vapors.[98]

3 Micro-sized polysilsesquioxanes

By optimization of the effective parameters, such as the amount of solvent, concentration of the monomer and catalyst, amount of surfactant, duration of the reaction, and the stirring speed, the 1–10 μm sized silsesquioxanes were prepared. Among these parameters, the increase in the concentration of the monomer, the duration of the reaction and the amount of catalyst increased the final size. While the decrease in the amount of solvent, the concentration of the surfactant and the stirring speed increased the final size of the silsesquioxanes, with the intense of the stirring speed and monomer concentration being more intense than the other parameters. Therefore, in general, supersaturation of the monomer concentration 0.4–1.0 mol L^{-1}, a long reaction time up to 96 h, a high amount of catalyst, a reduced amount of solvent, a low concentration of surfactant 3.60–3.20 g, and maintaining a the slow stirring rate of 400–100 rpm,[27,47,63,99,100] allows the seed to grow larger, resulting in the micro-sized silsesquioxanes.[49] Thus, by following this streamlined mechanistic behavior, the bridged, ladder-like, and intermixed silsesquioxane structures were produced by researchers.[23,39,101,102] Along with size control, the different silsesquioxane structures were generated by using their respective precursors and other necessary reaction conditions. These are shown in Fig. 14 to illustrate the relationship between size control and their respective geometries.

3.1 Bridged silsesquioxanes

The bridged shape micron-sized silsesquioxane materials are a useful part of the family of bridged compounds. Different compounds of this class with Q8 structures were prepared by combining bridged structure siloxanes–silsesquioxane with different allyl alcohols through a hydrosilylation process. A novel functional filler that is easy to modify and capable of forming covalent bonds with the polymer matrix was recently reported. The typical applications of this material as part of the polyurethane-based hybrid materials were analyzed. The preparation of different siloxane–silsesquioxane resins by changing the amount of SiH groups, named SiHQ-2, SiHQ-4, and SiHQ-8 (Fig. 15a), was performed.

For this, different types of composites, based on polyurethane (PU) were synthesized using the facile reaction of the 3-hydroxypropyl groups of a siloxane–silsesquioxane resin with 1,6-hexanediol and 1,6-diisocyanatohexane, named R2, R4, and R8. By experimentation it was proved that even with small amounts of filler, the PU based composite[103] exhibited enhanced thermal and mechanical properties, hence the proposed materials were considered to be a useful substitute for different silsesquioxane derivatives.[101] Salicylate composite sunscreen micro or sub-micron sized particles prepared using a modified Stöber process and oil/water microemulsion polymerization were employed to analyze the effects of the incorporation methods on UV safety, UV stability, and dye leaching by Tolbert *et al.* The investigations showed that in general, covalent incorporation can minimize leaching and photodegradation by necessary consolidation of the bridging to separate the sunscreen and any photoproducts on the skin. Fig. 15b shows a significant improvement in the UV-vis absorbance by a bridged silsesquioxane supported curcuminoid. Before the modification the curcuminoid particles demonstrated normal behavior for UV absorption, but after modification with silsesquioxanes the performance is enhanced significantly. Even the decrease in the absorption behavior was not as sharp as in the native curcuminoid, but after 2 h it decreased more than normal. After 3 h the trend became normal and finally ended with a little decrease. From the point of view of the ultraviolet protection ability, salicylic acid and curcumin particles were classified into a wide range and rated from moderate to advanced. This revealed the effectiveness of the merging method by describing the prospects of the bridging silsesquioxane, which is a striking technique for sunscreen protection, stabilization, and isolation. This effective model can eliminate the phototoxicity and photodegradation problems associated with existing sunscreens.[39]

3.2 Ladder-like silsesquioxanes

The ladder-shaped silsesquioxane materials in the micrometer size range are considered to be thermally stable and have good self-healing and anti-scratch properties. Some ladder-like polysilsesquioxanes with phenyl and methacryloxypropyl (LPMA)

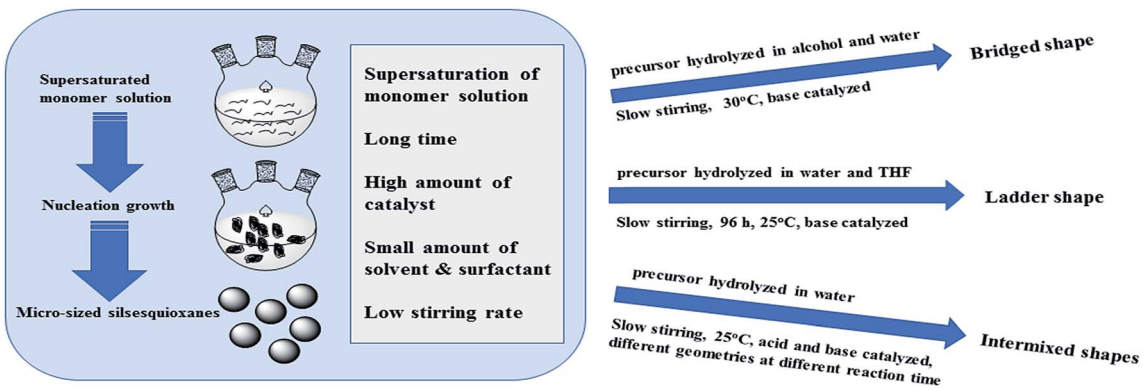

Fig. 14 A concept diagram of different micro-sized silsesquioxanes and their size control.

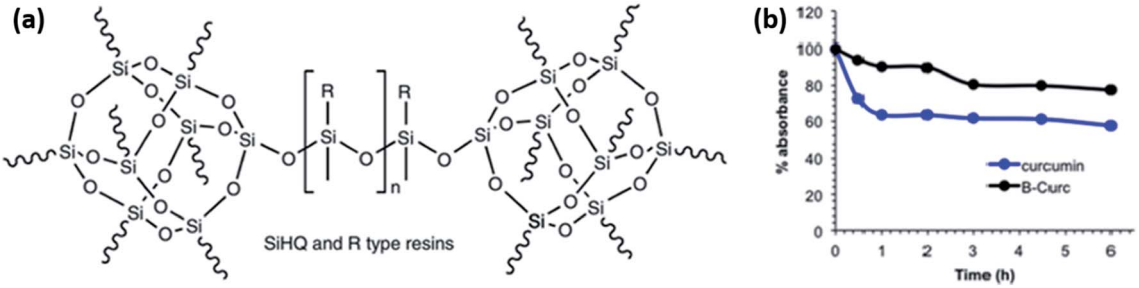

Fig. 15 (a) Structures of the organosilicon compounds. In which R = H for SiHQ-2, SiHQ-4, and SiHQ-8 resins before functionalization, or R = for R2, R4 and R8 functionalized resins $n = \sim1$, ~3 or ~7 for SiHQ-2, and R2, SiHQ-4 and R4, SiHQ-8 and R8 resins respectively. Adapted with permission from ref. 101 copyright 2018, Springer Nature. (b) UV-vis absorbance spectra for simple curcuminoid and bridged silsesquioxane supported curcuminoid samples exposed for 6 MED, which details UV-induced degradation over time for each sample (140.4 J cm^{-2} = 1 MED). Adapted with permission from ref. 39 copyright 2016, American Chemical Society.

groups have been modified to enhance the coating performance. These were constructed by careful tailoring of the methacryloxypropyl and phenyl groups by adjusting their molar ratios. Here, the C=C bonds of the methacryloxypropyl group were utilized for the polymerization reaction of the LPMA chains while the phenyl group was incorporated into the silsesquioxanes chains to make them robust and strong (Fig. 16).

For this, the base condensation reaction followed by a hydrolysis process was performed by using specific amounts of 3-methacryloxypropyl-trimethoxysilane (3-MPTS) and phenyltrimethoxysilane monomers.[102] Afterwards, LPMA solutions (1 wt%) and Irgacure 184 were both dissolved in THF solution to check the crosslinking behavior during the curing process of the LPMA solutions. A similar type of hydrolysis process was implemented for the preparation of a single-component ladder-like polysilsesquioxane and the resulting material exhibited improved self-healing Diels–Alder kinetics and mechanical properties. For this purpose, three different UV-curable functional groups (cyclohexylepoxyethyl, acryloxypropyl, and glycidoxypropyl) were used with a 20 mol% copolymer ratio. With these UV curing functions, the thermal response properties of the dienes and dienophiles were not affected when they were introduced to the same inorganic skeleton in a one component coating formulation. By doing so, these materials were able to exhibit smart recovery of the tough bulk (pencil hardness after 6 h) and of the mechanical properties of the nano-scale modulus (modulus of elasticity > 9 gpa). In addition, the excellent thermal properties (>400 °C), optical properties (transmittance > 95%), and solution processability of these materials provides great hope for incorporation into optoelectronic devices.[99]

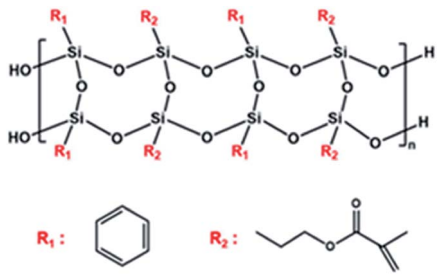

Fig. 16 The chemical structure of ladder-like polysilsesquioxane with the phenyl (R1) and methacryloxypropyl (R2) functional groups. Adapted with permission from ref. 102 copyright 2018, Elsevier.

3.3 Unspecified geometric silsesquioxanes

Some versatile and multipurpose micro-sized PSQs with unspecified or intermixed geometries were fabricated and modified for extensive applications. Herein, Yang *et al.*, synthesized PMSQ microspheres of different sizes using a two-step sol–gel process which disperse well into the oil phase as single spheres. Among the different sizes, the 2 μm PMSQ microspheres were found to be the best for the waxy crude oil sample A (wax content 25.2 wt%) while 5 μm PMSQ microspheres were the best for waxy crude oil sample B (wax content 16.5 wt%). A 200 ppm dosage of PMSQ microspheres was proved as a fit for both crude oils A and B. Analysis revealed that a small dose of PMSQ microspheres significantly improved the flow performance of the two distinctive waxy crude oils. The most important performance characteristics observed from adding PMSQ microspheres was the considerably reduced gelation point, storage modulus G', and loss modulus G'' of the oil sample, indicating that the PMSQ microspheres had an inhibitory effect on the viscoelastic development of the oil samples. Similar experiments with these crude oils confirmed that these PMSQ microspheres considerably change the flow performance of the waxy crude oil without taking part in the precipitation process to form waxy crude oil crystals.[23] A similar type of hydrophobic silsesquioxane materials were made by using the fluoride rearrangement reaction to prepare mixed functional silsesquioxane-siloxane copolymers for hydrophobic and robust coatings. The silsesquioxane–siloxane system of octamethylcyclotetrasiloxane (D4), dodecaphenylsilsesquioxane $[PhSiO_{1.5}]_{12}$ (DDPS), methacryloxypropyltrimethoxysilane (MAS), and tridecafluoro-1,1,2,2-tetrahydrooctyl)triethoxysilane (PFS) with silicon dioxide in different combinations was used for this purpose. Thereby F^- was used as a catalyst to rapidly balance all $RSiO_{1.5}$ units in the coating system. To obtain a better understanding and to optimize the conditions for these versatile materials, the relationship between the durability, thermal properties, hydrophobicity, and composition was discussed.

These polymers were formed by the evaporation of moisture and solvents using the solvent drying method. Another aspect of the system was that if the coating does not meet the target performance in the first test, only one or two components that are expected to produce a better performance can be replaced to modify the coating solution and allow the system to equilibrate before the next application. This unique feature of this material was observed and there are few or no other coating systems that exhibit this kind of *in situ* modification.[32] Another interesting type of hydrophobic PSQs, named the phenyl (PSQ-Ph), cyclohexyl (PSQ-Cyc6), hexyl (PSQ-C6), and undecanyl (PSQ-C11) silsesquioxanes, were prepared using a simple reaction of PSQ-NH_3CL with the corresponding hydrophobic carboxylic acid chlorides (benzoyl, cyclohexane carbonyl, heptanoyl, and dodecanoyl chlorides) respectively. All of the reactions were carried out using water and DMF as a mixed solvent in the presence of triethylamine and all were soluble in chloroform and hydrophobic in nature. These PSQs were used to prepare organic polymer hybrid membranes with hydrophobic PSQ by drying the chloroform solution of the mixture. The hybrid films made using this combination of poly(methyl methacrylate) (PMMA/PSQ-C6, PMMA/PSQ-C11), and polystyrene (PS/PSQ-Ph) were highly transparent. A trend was observed that when the amount of PSQ-Ph was increased, the thermal stability also increased significantly. From the above described properties, the hydrophobic PSQ synthesized in this research could have broad application prospects in academia and industry.[104] In the field of catalysis the micrometer sized poly(chloropropylmethyl)silsesquioxanes (PCMSQ), which have good catalytic properties were synthesized using water and methanol as a solvent. For this 3-chloropropyltriethoxysilane (CPTES) and MTMS with molar ratios of 5 : 5, 6 : 4, and 7 : 3 were used and the reaction was carried out by a sol–gel process with the base as a catalyst. To give an idea of the maximum yield of PCMSQ, an elemental analysis technique was used. This analysis revealed that MTMS : CPTES with a molar ratio of 6 : 4 was the best for the synthesis of PCMSQ. When *ortho*-phenylenediamine (opda), ethylenediamine (en), 2-imidazolidinethion (imt) and diethylenetriamine (dien) were refluxed with chloropropyl groups, these were converted into different amines. The PCMSQ grafted with a dien and amine were then utilized for the epoxidation of *cis*-cyclooctene with high contents of metal and to support the $MoO_2(acac)_2$ complex respectively.[105] For the first time, a platinum based styrene-divinylbenzene copolymer Pt/SDB-catalyzed multiphase catalytic system for silsesquioxane $(HSiMe_2O)(i\text{-}Bu)_7Si_8O_{12}$ was studied. It was found that this copolymer Pt/SDB is an effective addition system of silicon hydride in many examples of these two families. Their characterization results revealed that the reusability and activity of Pt/SDB were better than those obtained using the platinum catalysts already available, based on Degussa carbon. This catalyst has been proved to be highly tolerant and active to many other functional groups such as epoxy,[106,107] COOR, Br, OH, formyl, silyl and so forth. Which is why the usefulness of this catalyst makes it an important system for hydrosilylation, especially in the industrial production of functionalized silsesquioxanes.[108]

4 Applications

Generally, when the particle size of any material is in the nano range, the overall surface area increases. Owing to this, the surface to surface interaction of particles with the corresponding substrate increases which leads to better contact of the materials and thus the final properties are affected. The metal atoms bearing silsesquioxanes show a size dependent effect in their properties. When nanosized metal particles are attached to their compatible nanosized silsesquioxanes, the overall material shows a better performance for some specific applications. Firstly, the metal nanoparticles exhibit specific absorption, transmittance and fluorescence wavelengths owing to the highest occupied molecular orbital–lowest unoccupied molecular orbital (HOMO–LUMO) band gap changes and secondly, the small size of the silsesquioxanes proved to be more favorable for precipitation and desorption purposes in those materials in which detection, fluorescence, and catalytical properties are required.[60,67,86,94,109–111] In addition, the micro-sized silsesquioxanes disperse well in the oil phase as a single sphere compared to their nano-sized counterparts. Some materials showed a better performance when silsesquioxane particles were incorporated into them owing to their micro size. When these silsesquioxane micro particles are mixed with waxy crude oils, they formed a floc and inhibited the continuous crystal network growth of the oils. This discontinuous crystal network leads to an improvement in the compactness, flow behavior, viscous modulus, elastic modulus, gelation point, yield stress, and their apparent viscosity. Furthermore, when these micro spheres are mixed with a solid substrate, they increased their hydrophobicity and generated a delay in the thermal degradation process and enhanced the thermal stability.[23,38,47,87,104]

4.1 Anti-scratch and hardness

Different types of silsesquioxane materials have diverse properties and several general features which characterize them, however ladder like poly silsesquioxanes are unique in showing scratch resistance and hardness. The hardness of a series of LPSQs containing the UV curable MA ladder like silsesquioxanes LMAR films (R = N, naphthyl: P, phenyl; C, cyclohexyl; Pr, propyl; and H hexyl) were examined using the penetration test while applying normal force (Fig. 17). All of the films featured good mechanical properties and optical transparency with a good degree of colorlessness. The mechanical properties of these films were influenced by the chain stacking density of the siloxane skeleton and the chain stiffness of the organic functional group R, but the chain stiffness effect dominated the chain stacking density effect. The LMAN film consisting of a naphthyl group showed the maximum scratch resistance, modulus of elasticity and hardness owing to the increased chain reinforcement imparted by its high aromaticity.[80]

In order to assess the healing capability of different ladder-like polysilsesquioxanes (as elaborated in Section 2.1.2), LPCSQs were characterized and thermally repaired at 110 °C

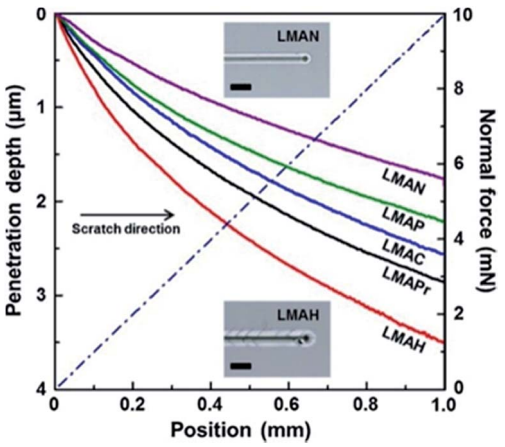

Fig. 17 The penetration depth profiles for a scratch length (1 mm) of the UV cured LMAR films. Inset images show the optical microscopy images of the LMAN and LMAH film surfaces after the scratch test (scale bar = 10 μm). Adapted with permission from ref. 80 copyright 2018, Elsevier.

after a scratch was marked. Fig. 18 shows the scratch samples in which the crack size was almost 100 μm.

After 5 min of heat treatment at 110 °C, the scratches were cooled to the cold-impact state in air, and the scratches were healed completely. Compared with other self-healing materials,[90,112] the reaction time of the DA reaction was basically the same. However, in the rDA reaction, the reaction temperature of LPCSQs-rDA was lower than that of the other materials, and the complete healing time was shorter. In another work Xu *et al.*, mentioned a thermally healable POSS nanocomposite that heals completely by performing a rDA reaction at about 155 °C for 30 min and DA reaction at 90 °C for 18 h.[113] In the rDA reaction, the reaction time of LPCSQS was six times faster than that of Xu's reported self-repairing materials. The recycling process was repeated three times in succession, which showed that the process had a good recyclability.[81] The different ladder-like PSQs with different ratios of phenyl and methacryloxypropyl group LPMA films (Table 2) showed an interesting behavior against an external load. Compared with the films that were mainly composed of phenyl, the scratch widths of the LPMA films with larger proportions of methacryloxypropyl were narrower.

The LPMA82 and LPMA91 films (having lower methacryloxypropyl contents) showed fragile behavior under external loads as more cracks were observed on their surfaces as shown in Fig. 19a and b.

The surface mechanical properties of the solidified LPMA films were closely related to the cross-linking properties of the LPMA solution during solidification. It is important to understand the development of curable coatings in the entire curing process by clarifying the role of the functional groups and the configuration of the cross-linking structures in various photocuring or thermal curing systems.[102]

4.2 Light absorption

Many modified silsesquioxane materials have been prepared for the purpose of photoabsorption, fluorescence, light sensing,

Table 2 LPMA samples with various molar ratios of phenyl and methacryloxypropyl functional groups. Adapted with permission from ref. 102 copyright 2018, Elsevier

	Molar ratio of side groups[a] (mol%)			
Sample	Phenyl	Methacryloxypropyl	M_w[b] (kg mol^{-1})	Remark
LPMA19	10	90	7	Liquid type
LPMA28	20	80	9	
LPMA46	40	60	15	
LPMA64	60	40	24	Solid type
LPMA82	80	20	13	
LPMA91	90	10	9	

[a] Calculated by ^{1}H NMR. [b] Analyzed by GPC using polystyrene standard.

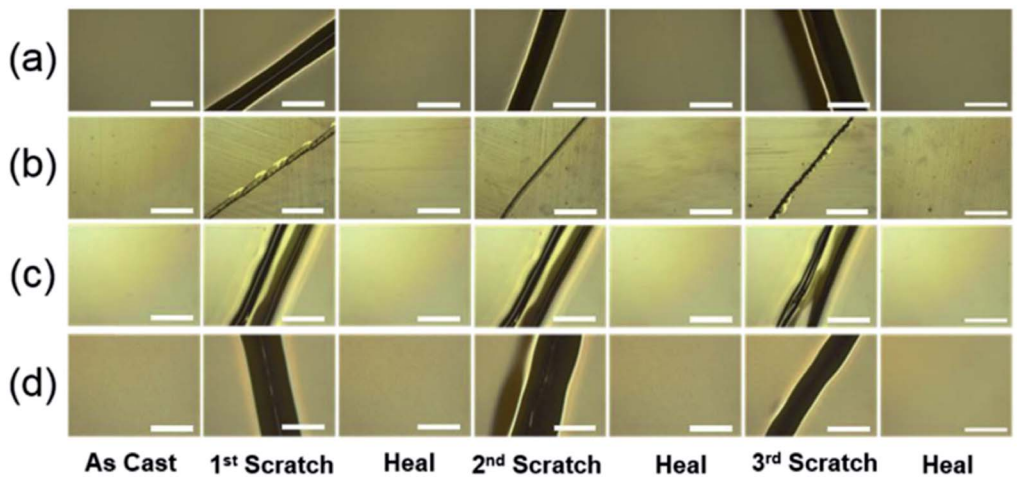

Fig. 18 Optical microscopy images of: (a) LPCSQ55; (b) LPrPCSQ244; (c) LHPCSQ244; and (d) LDPCSQ244 films coated on glass substrates. The DA–rDA cycles were repeated sequentially three times; scale bars = 100 μm. Adapted with permission from ref. 81 copyright 2017, Elsevier.

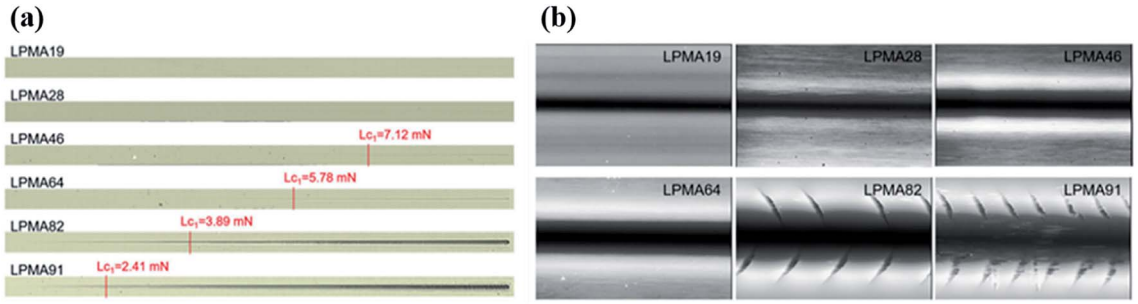

Fig. 19 (a) Panoramic images using an optical microscope (100× magnification). (b) Final shapes of the residual depths visualized using AFM. Adapted with permission from ref. 102 copyright 2018, Elsevier.

and related phenomenon. Owing to these capabilities, they have fascinating applications for cancer treatment, metal sensing, and fluorescence. Here, the BSNPs were used as powerful multifunctional nanosystems in cancer cells by combining the TPE-PDT technique and ultra-bright fluorescence imaging technology. The two-photon fluorescence quantum yield of the nanomaterials was measured and it showed that the two-photon absorption cross sections of all synthesized nanoparticles were higher than those of their precursors. These NPs were used as powerful multifunctional nanosystems in cancer cells by combining TPE-PDT and ultra-bright fluorescence imaging technology. Adding gold nanospheres to the BSNP matrix significantly improved the *in vitro* fluorescence related to the photophysical studies (Fig. 20). Finally, compared with BSNP, the gold-doped BS nanosystem increased the killing rate of TPE-PDT cells by 20–25% by applying an equal amount of irradiation, indicating that BSNP and gold-doped BSNP are very promising cancer treatment methods.[60]

On the other hand, the same TPE-PDT technique was used for the treatment of breast cancer cells, MCF-7, by preparing bridged silsesquioxane NPs from a tetrasilylated porphyrin (BSPOR) and tetrasilylated phthalocyanine (BSPHT) through

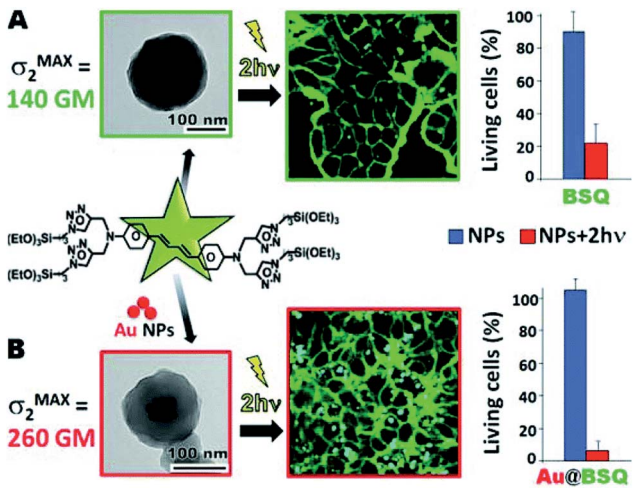

Fig. 20 Application of BSQ and gold core BSQ shell NPs obtained by using the TPE-PDT technique and imaging in the treatment of cancer cells. Adapted with permission from ref. 31 copyright 2016, Wiley.

click chemistry. When characterizations for the configuration and morphology of the nanoparticles were made, the existence of a photosensitizer was confirmed. The nanoparticles were cultured with breast cancer cells MCF-7 for 20 h. Before the imaging experiment, the cell membrane was stained with an orange plasma membrane for 15 min. By using a Carl Zeiss confocal microscope, two-photon imaging was performed at a low laser power (6% input). Endocytosis of the NPs was clearly observed in the merged image (Fig. 21a) and their tracking efficiency in cells was verified.

When this technique was applied to cancer cells *in vitro* it showed amazing results. First, the cells were irradiated at 800 nm at a high laser power (100% input using a Carl Zeiss confocal microscope). After 48 h a simple MTT assay control (a colorimetric assay for assessing the cell metabolic activity) was performed. Surprisingly, by using the same experimental conditions, BSPHT killed 21% of the cancer cells, while 86% of the cancer cells were eradicated by BSPOR (Fig. 21b).[67] In another study, ultraviolet and fluorescence irradiation were used to analyze the Hg^{2+} sensing by POSS particles (T10Rh) modified by rhodamine hydrazide receptors. A comparison was performed by incorporating alkali, alkaline earth, other metals[114–116] and Hg^{2+} ions with T10Rh. The selectivity of T10Rh to Hg^{2+} was higher than that of the other foreign ions. Owing to the HOMO–LUMO specific band gap of the metals in the nano scale, the absorption and fluorescence wavelengths become size dependent.[109] As such, nanosized mercury particles are well suited to the absorption of wavelengths from 530–650 nm, therefore when Hg^{2+} was added to the solution, the fluorescence emission was enhanced significantly at 580 nm. T10Rh showed that the fluorescence reaction increased rapidly only with the increase of the Hg^{2+} concentration as shown in Fig. 22a. Meanwhile, Fig. 22b shows the colorimetric reaction of T10Rh to Hg^{2+} standard samples, which changes from colorless to pink. This was demonstrated in skin whitening cream with and without Hg^{2+} standard addition, this sensor for Hg^{2+} has a high potential for practical applications in environmental samples.

The color change of the sensor was obvious after the combination of Hg^{2+} with POSS and as the amount of Hg^{2+} used was only 0.63 ppb, which is lower than the permissible amount present in drinking water, it could be used in for *in situ* determination of Hg^{2+}. Using this concept, other researchers could

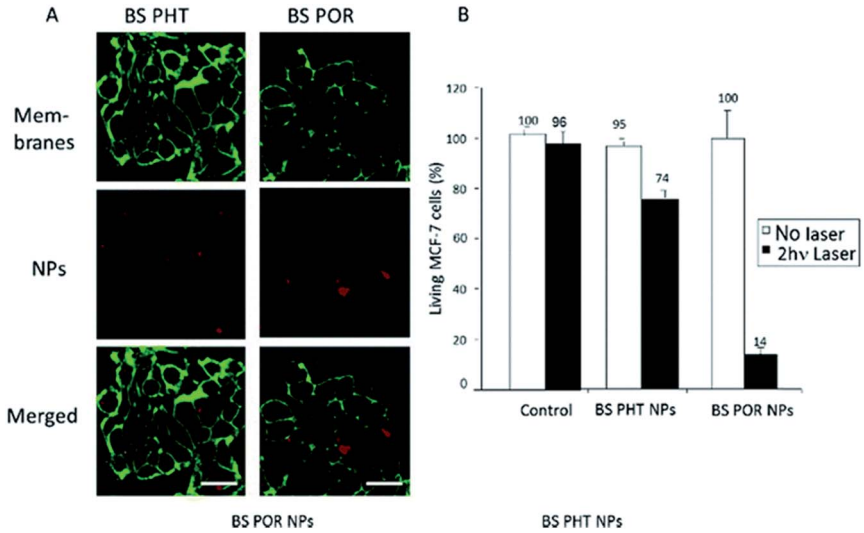

Fig. 21 (a) Two-photon confocal microscopy images of cells at 800 nm (BSPOR) and 750 nm (BSPHT). NPs incubated for 20 h with 80 μg mL^{-1} of BSPOR or BSPHT. Scale bars = 10 μm. (b) TPE-triggered killing of cancer cells using BSPOR and BSPHT NPs (irradiated at 800 nm). Adapted with permission from ref. 67 copyright 2017, Wiley.

use POSS particles as core sensors with other metal ions, as they are more effective as simultaneous absorbers and sensors than traditional silica absorbers.[86] Chen *et al.*, prepared porous near infrared photoluminescent POSS-based materials by hydrosilylation and the polymerization of vinyl POSS with hydrogen-terminated silicon nanocrystals (ncSi:H). The modified particles had a high pore volume and surface area, which were in the range of 290.5–1047.2 m^2 g^{-1} and 0.64–1.17 cm^3 g^{-1}, respectively (Table 3). The pore size was 6.08–3.54 nm, depending on the weight ratio of vinyl POSS to ncSi:H of the different samples, which is the most attractive feature of this material in the field of POSS based modified materials.

The analysis showed that the absolute quantum yield of near-infrared photoluminescence of the nanocomposites was almost independent of the weight ratio of vinyl POSS to ncSi:H. Fig. 23a shows the significant improvement in the absolute quantum yield (%) before and after the reaction of vinyl POSS with a different weight ratio of ncSi:H. This phenomenon can also be observed using the naked eye after UV exposure (Fig. 23b).

This work not only introduced the idea for the preparation of advanced porous POSS-based materials with ideal functions, but also provided application opportunities as delivery platforms, drug carriers, gas adsorption media, and catalyst carriers.[94]

4.3 Catalytic properties

After modification with silsesquioxane particles some metals and non-metals showed exciting catalytic properties as catalysts. The turn over frequency (TOF) is a suitable parameter for the comparison of the catalytic efficiency, which is why it was used here to compare the catalytic efficiencies of different systems. Herein, Mohapatra and his team successfully used a palladium metal nanoparticles supported with POSS (3 ± 1.5 nm size) for the catalysis of C–C coupling reactions (Fig. 24). This POSS material fabricated with Pd metal showed a high catalytic activity for the Suzuki–Miyaura cross-coupling reactions with a TOF of up to 1670 h^{-1}. These nanoparticles proved to be exceptionally stable as they remained unchanged for more

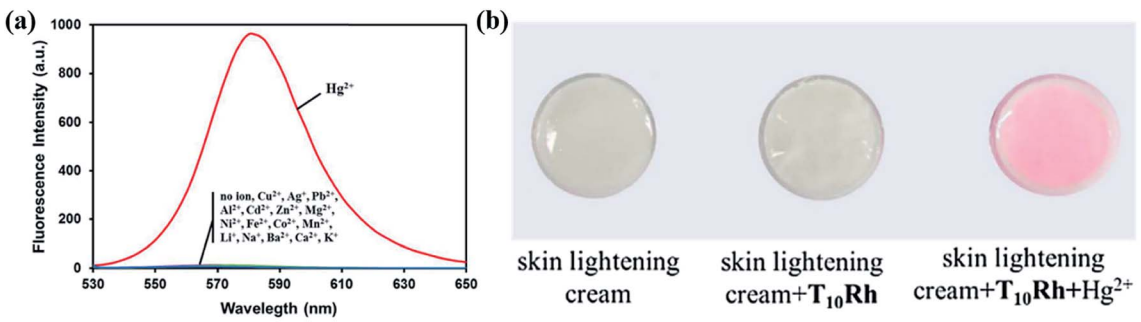

Fig. 22 (a) Fluorescence spectra (l_{ex} 520 nm) of T10Rh (1.00 mM) in 10% aqueous ethanol solutions with the addition of perchlorate salts of Hg^{2+}, Cu^{2+}, Ag^{+}, Pb^{2+}, Al^{3+}, Cd^{2+}, Mg^{2+}, Ni^{2+}, Fe^{2+}, CO^{2+}, Mn^{2+}, Zn^{2+}, Li^{+}, Na^{+}, Ba^{2+}, Ca^{2+} and K^{+} (21.3 mM). (b) Skin lightening cream without and after spiking with Hg^{2+}. Adapted with permission from ref. 86 copyright 2018, Elsevier.

Table 3 The surface area and porosity diagnostics of vinyl-POSS polymer composites with ncSi (VS = vinyl POSS + ncSi:H, VS-0 = pure vinyl POSS). Adapted with permission from ref. 94 copyright 2016, John Wiley and Sons

Sample	Weight ratio of ncSi:H to vinyl POSS	Surface area [$m^2\ g^{-1}$]	Pore volume [$cm^3\ g^{-1}$]	Mode pore size [nm]
VS 0	0	793.2	0.66	3.54
VS I	1 : 2	320.3	0.64	6.08
VS II	1 : 5	290.3	0.68	6.08
VS III	1 : 10	1047.2	1.17	4.89

than 10 reaction cycles without losing their activity. Additionally, the imidazolium functional group was also part of the POSS surface, it played a key role in the solubility properties of the Pd based POSS catalyst. The NHC groups of this catalyst system also play their part to stabilize the Pd nanoparticles that are liberated into the solution and act as an active homogeneous catalyst. This catalytical system and its method of use are convenient, low cost, environment-friendly and highly useful. Owing to nano-sized material and the convenience of this catalytic system, it can be assumed that other researchers in this field could further explore the other Pd-catalyzed reactions while carefully tuning the size, as a larger catalyst size can reduce its efficiency.[111]

In the same way, many molybdenum complexes have been reported for the catalytic epoxidation of alkenes with tetrabutylhydroperoxide TBHP. However, poly(chloropropyl-methyl) silsesquioxanes prepared by Mirzaee *et al.*, had better catalytic efficiency for the epoxidation of alkenes within specified conditions. Except for the last one, as shown in Table 4, the TOF values of other studies were lower than Modien-PCMSQ-2 (~48 h^{-1}). In addition, the TOF value was comparable to this reported catalytic scheme, which included molybdenum complexes supported on Schiff base functionalized boehmite nanoparticles (44 h^{-1}).[117]

In addition, the industrial application of this new catalytic reaction scheme has also been confirmed by the 20-fold scale-up catalytic epoxidation experiments.[105]

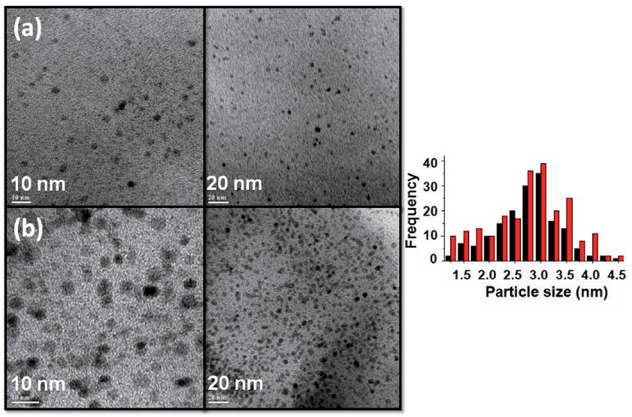

Fig. 24 Right: TEM images of the catalyst isolated from the Suzuki–Miyaura reactions after: (a) the 1st cycle; and (b) the 10th cycle. Left: Histogram obtained considering: 160 (black); and 200 particles (red). Adapted with permission from ref. 111 copyright 2016, John Wiley and Sons.

4.4 Hydrophobicity and thermal stability

Materials that have a high thermal stability and hydrophobicity are very important in various practical fields. In addition, if these materials act as fillers with other materials, it makes them more demanding. Highly hydrophobic and thermally stable silsesquioxane materials are renowned in this field.[122] Therefore a new solvent resistant PMSQ aerogel was developed for the first

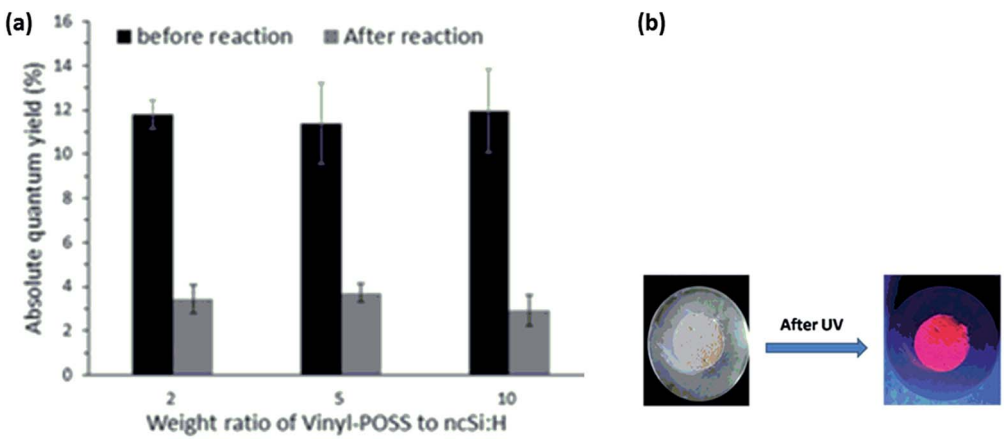

Fig. 23 (a) Effect of weight ratio of vinyl-POSS to ncSi:H on the absolute quantum yield. (b) Modified POSS before and after UV exposure. Adapted with permission from ref. 94 copyright 2016, John Wiley and Sons.

Table 4 Comparison of the catalytic epoxidation of *cis*-cyclooctene with tetra-butylhydroperoxide by using different molybdenum complexes[105]

Sr. No.	Catalyst	Turn-over frequency (TOF)	References
1	Dioxo molybdenum complex supported on an organic copolymer	5 h^{-1}	118
2	Molybdenum complex supported on nanomagnetite	19 h^{-1}	119
3	Molybdenum Schiff base complex supported on amino functionalized mesoporous materials	25 h^{-1}	120
4	Molybdenum and vanadium Schiff base complexes supported on boehmite nanoparticles	44 h^{-1}	117
5	Molybdenum complex supported on PCMSQ-2	48 h^{-1}	105
6	Molybdenum complex supported on multi-walled carbon nanotubes	55 h^{-1}	121

time under the action of low dose CTAB surfactants and MTMS. The advantageous aspect of these CTAB modified PMSQ aerogels is that their water contact angle increased to more than 160°. The results showed that this material achieved super hydrophobicity, which makes it an ideal waterproof solvent adsorbent as shown in Fig. 25.

Whereas, CTAB modified PMSQ aerogels with a higher specific surface area and a 0.002 molar ratio of CTAB/MTMS (C/M) have a higher adsorption capacity compared to other C/M mole ratio aerogels. The research revealed that low dose CTAB modified PMSQ aerogels not only have solvent resistance but also have industrial potential to adsorb organic solvents. This study also provided the feasibility for developing other solvent-resistant materials by adding CTAB surfactants at low dosages.[38] The hydrophobicity or superhydrophobicity of the coating is generally maximized at the expense of the wear resistance and *vice versa*. Therefore, Krung and colleagues synthesized siloxanes/silsesquioxane coatings through a simple protocol of rearrangement reactions using an F^- catalyst. This reaction scheme has the capability to maximize the water repellency and durability of the resultant coating system. Fig. 26a shows the reported siloxanes/silsesquioxane system with silicone dioxide DDPS + D4 + PFS + MAS + SiO_2 (mentioned in Section 2.3.3) which exhibited an outstanding water contact angle (WCA) at about 150 wear cycles. At first the WCA of all materials was not significantly different, but with the increase in wear cycles the difference became larger. At about 150 cycles, the DDPS + D4 + PFS + MAS + SiO_2 system showed the maximum WCA and achieved superhydrophobicity compared with the other materials.[123] Furthermore, after this all of the materials showed a small decrease in the WCA at a higher number of wear cycles, as it exceeds the limit of the nature of the materials. The robustness of the siloxanes network was achieved by the removal of the solvent and the F^- scrambled network was frozen in place of the solvent. When the organic contents were optimized into these siloxane networks, they showed high thermal stabilities of greater than or equal to 340 °C and sometimes even increased up to 460 °C.[32] Whereas, the thermal stability of the silsesquioxanes was determined by preparing composite films of the different PSQs (mentioned in Section 2.3.3) with PS. The first thermographic analysis of simple PSQ-C11, PSQ-C6, PSQ-CyC6, and PSQ-Ph was performed and showed that the best performance was exhibited by PSQ-Ph compared with the other PSQs (Fig. 26b).

Although phenyl, cyclohexyl, and hexyl side chain groups have an equal number of carbon atoms the thermal decomposition temperature of the phenyl containing PSQ was the highest among the three PSQs owing to the existence of the thermally stable phenyl side chain groups. Meanwhile, the thermal decomposition temperature of PSQ-C_6 was higher than that of PSQ-CyC_6, because the side chains of PSQ-C_6 can be arranged regularly owing to its linear structure. On the contrary, the PSQ-CyC_6 side chain has a large ring structure, which is difficult to arrange properly and easy to crack. PSQ-Ph was then used with PS and different films were made with different ratios to explore the thermal performance of these films (Fig. 26c). The composite PS/PSQ-Ph 1 : 3 (25/75) showed the maximum thermal stability which indicated that high contents of phenol made the material hard and tough against heat.[104]

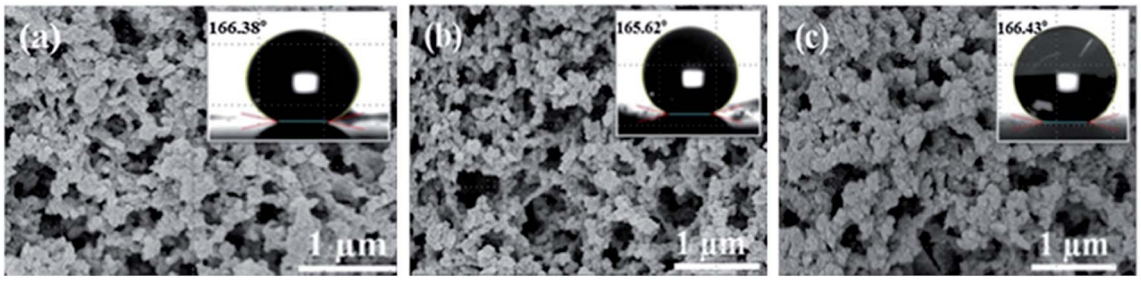

Fig. 25 Field emission scanning electron microscopy (FESEM) and contact angle images of the CTAB-modified PMSQ aerogels with C/M molar ratios of: (a) 0.001; (b) 0.002; and (c) 0.004. Adapted with permission from ref. 38 copyright 2017, Elsevier.

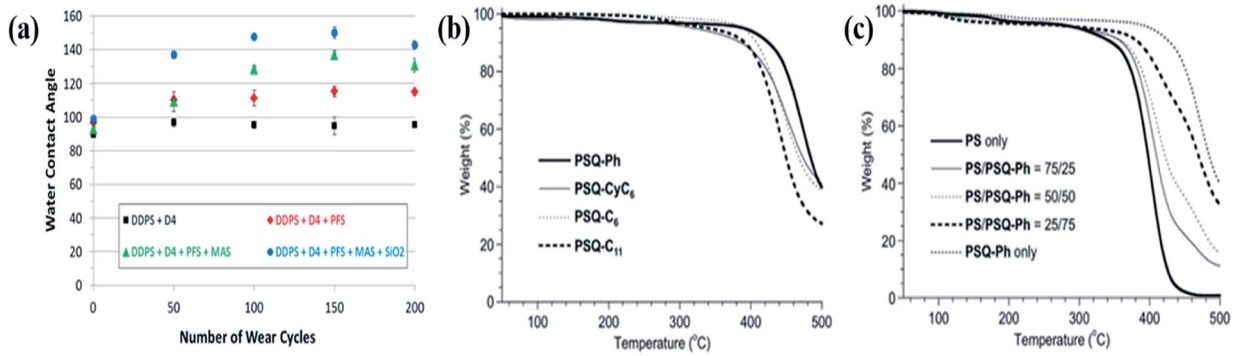

Fig. 26 (a) WCA of hybrid coatings *versus* wear cycles with 100 g weighted 2000 grit sandpaper. Adapted with permission from ref. 32 copyright 2017, American Chemical Society. (b) Thermal gravimetric analysis (TGA) thermograms of PSQ-Ph, PSQ-CyC6, PSQ-C6, and PSQ-C11; (c) thermograms of PS, PSQ-Ph, and the hybrids of PS/PSQ-Ph (75/25), PS/PSQ-Ph (50/50); and PS/PSQ-Ph (25/75) under a nitrogen flow. Adapted with permission from ref. 104 copyright 2016, Elsevier.

4.5 Surface area and mechanical properties

Some silsesquioxane based aerogels, layered materials, and epoxy resins show outstanding properties related to the surface area, hardness, and good mechanical strength. Huo *et al.*, prepared a waterborne alkyd resin and epoxy resin (AR/ER) and examined their effect on 3-glycidyloxypropyl-POSS (G-POSS). Glass fiber reinforced nanocomposite laminates with a 3 mm thickness were prepared by using water-borne ER/AR resin mixtures with different G-POSS contents as raw materials while maintaining the mass ratio of ER/AR at 1 : 1. Finally, the mechanical properties of the composites were measured which show a clear difference owing to the addition of G-POSS as compared with simple methyltetrahydrophthalic anhydride (MTHPA) (Table 5).

For G-POSS, when the contents were 6 wt%, the laminate shows the best mechanical properties, which explained why the system has such a good distribution and compatibility.[54] Lei *et al.* prepared PMSQ aerogels by using ammonia as a surfactant with a controlled size from 10 to 40 nm which showed outstanding properties related to the surface area and flexibility. The high amount of ammonia surfactant controlled the size which leads to a better performance. Owing to the nano-sized skeleton, the interstices and space were arranged in such a way that overall the material becomes mechanically strong as well as flexible. This specific size allowed the aerogels to be able to bear the external force and to maintain the shape. Fig. 27a and b shows the smooth decrease in the shrinkage and density with the increase in the dose of ammonia.

When the particles move close to each other, the specific surface area decreased from 615.0 to 382.2 $m^2 g^{-1}$. The decrease in the radical shrinkage was from 7.75% to 3.29% and correspondingly the density decreases from 0.144 to 0.121 g cm^{-3}. By comparing the mechanical properties of A6 and X6 (X = xerogel, after replacing the ethanol in the aerogel with *n*-hexane), it becomes clear that owing to the strong skeleton, the flexibility of X6 improved with a significant decrease in the Young's modulus as well, as an increase in the resilience from 65% to 80% as shown in Fig. 28a. Using this method, crack free aerogels have been obtained by using a high ammonia concentration and an atmospheric pressure drying method.[87]

In addition to these PMSQ based aerogels, thermally treated silsesquioxanes (TSQ) grafted on graphene oxide with soluble polyimides (SPI/TSQ@GO) nanocomposites have shown an effective enhancement in the elongation at break and the tensile strength (Fig. 28b) with clear identification of the yield point in the tensile stress–strain curves. In comparison to the native SPI, a steady increase in the elongation at break (from 7.18% to 20.97%) and in the tensile strength (from 67.6 to 86.7 MPa) were observed when the dose of TSQ@GO was enhanced from 0 to 2.0 wt%. This improvement reached the maximum at 2.0 wt% (optimal value of SPI/TSQ@GO) with a three-fold increase in the elongation at break and a 1.3 times

Table 5 Mechanical properties of AR/ER (1/1) with different content of G-POSS. Adapted with permission from ref. 54 copyright 2018, Taylor & Francis

Samples (G-POSS wt%)	Impact strength (kJ m^{-2})	Standard deviation	Tensile strength (MPa)	Standard deviation
0	83.18	±2.27	196.05	±0.53
1	92.81	±1.22	195.98	±0.75
3	94.58	±0.27	187.03	±0.29
6	136.19	±0.52	181.02	±0.93
9	83.21	±0.49	168.82	±0.79
12	60.31	±0.41	147.53	±0.42
MTHPA	67.51	±2.28	158.28	±0.15

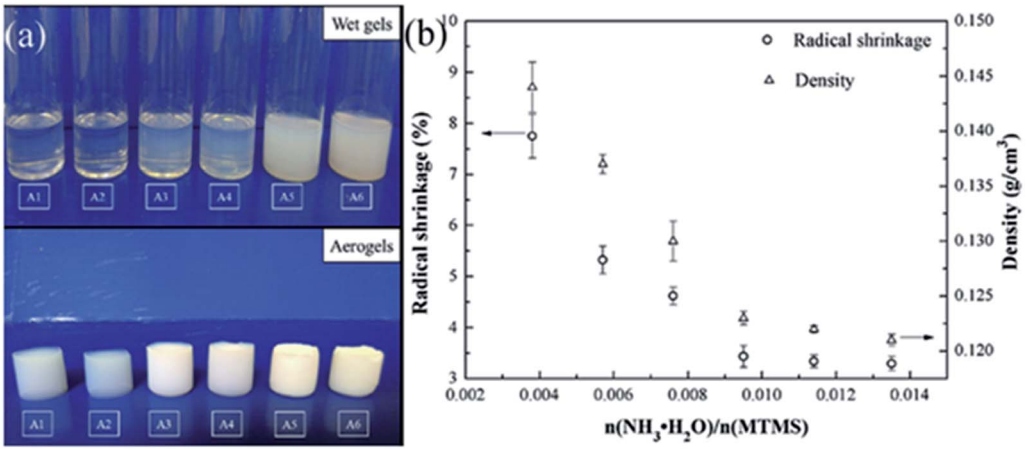

Fig. 27 (a) Photographs of the monolithic silica wet gels and aerogels (A1–6 = aerogels containing ethanol as a solvent with a different concentration of NH_3); and (b) the radical shrinkage, density of aerogels with various amounts of ammonia. Adapted with permission from ref. 87 copyright 2018, Elsevier.

enhancement in the tensile strength.[124] This indicates that these new materials as a whole could be used in general applications, such as for use as lightweight bulking materials, high performance fillers, and insulation materials.

5 Summary and outlook

Herein, we have summarized the recently developed PSQ-based functional materials. On the basis of their nano and micro size, these PSQs present a wide variety of novel modified materials. The key factor of the size was controlled by the amount of surfactant, the concentration of the monomer, the type of solvent, and the stirring speed within a specific reaction time. The resulting nano-sized PSQs have a good ability for proper dispersion in the substrate, and were in the form of bridged, ladder-like, cage shape and other geometries that have been modified by methacrylates, long alkyl chains, cyclic compounds, rhodamine hydrazide, phosphonic acid, glycidyloxypropyl, Au, Ge, Ni, Cu, Sc, other organometallic functional moieties and so forth. On the other hand, micro-sized PSQs which have the capability to provide a greater surface area for guest functional moieties have been modified using allyl alcohol, polyurethane, salicylate, curcuminoid, methacryloxypropyl, cyclohexylepoxyethyl, dodecanphenyl, polycholoropropyl-methyl, and some aliphatic cyclic compounds. Owing to their tough and multifunctional nature, these PSQs altogether were utilized as a hard coating material for anti-scratch materials, as photon emitters for cancer treatment, UV absorbers for heavy metal detection, as a good recyclable catalyst with PD which has a high TOF, and as a sunscreen agent. This monolithic variety of PSQs with multiple retention mechanisms and interesting applications will be in high demand in the future.

Conflicts of interest

The authors declare that there is no conflict of interests regarding the publication of this paper.

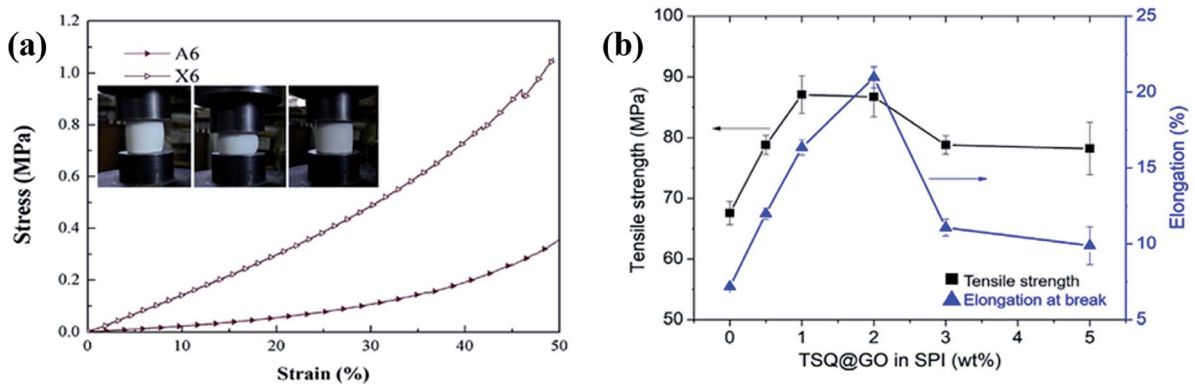

Fig. 28 (a) Compressive stress *versus* strain curves of the resulting aerogels. Adapted with permission from ref. 87 copyright 2018, Elsevier. (b) Effects of the loading of TSQ@GO on the tensile strength and elongation at break. Adapted with permission from ref. 124 copyright 2019, Elsevier.

Abbreviations

PFS	(Tridecafluoro-1,1,2,2-tetrahydrooctyl) triethoxysilane
MTICl	1-Methyl-3- [3-(triethoxysilyl)propyl]imidazolium chloride
CPTES	3-Chloropropyltriethoxysilane
G-POSS	3-Glycidyloxypropyl-POSS
3-MPTS	3-Methacryloxypropyl-trimethoxysilane
HNTf2	Bis(trifluoromethanesulfonyl)imide
BTMSPA	Bis[(3-trimethoxysilyl)propyl] amine
BSNPs	Bridged silsesquioxane nano particles
BSPHT	Bridged silsesquioxane phthalocyanine nano particles
BSPOR	Bridged silsesquioxane porphyrin nano particles
CLMSs	Cage-like metallasilsesquioxanes
CTAB	Cetyltrimethylammonium bromide
DA	Diels–Alder reaction
DDPS	Dodecaphenylsilsesquioxane
ER	Epoxy resin
GO	Graphene oxide
HOMO–LUMO	Highest occupied molecular orbital–lowest unoccupied molecular orbital
LPCSQ	Ladder-like poly(*n*-propylpyrrole-*co*-cyclohexenylethyl)silsesquioxane
LMAC	Ladder-like polysilsesquioxane methacrylate cyclohexyl
LMAH	Ladder-like polysilsesquioxane methacrylate hexyl
LMAN	Ladder-like polysilsesquioxane methacrylate naphthyl
LMAP	Ladder-like polysilsesquioxane methacrylate phenyl
LMAPr	Ladder-like polysilsesquioxane methacrylate propyl
LMSH	Ladder-like silsesquioxanes methacrylate siloxane hybrid
LPMA	Ladder-like silsesquioxanes of phenyl and methacryloxypropyl
MOFs	Metal–organic frameworks
MSH	Methacrylate siloxane hybrid
MA	Methacryloxypropyl
MAS	Methacryloxypropyltrimethoxysilane
MTHPA	Methyltetrahydrophthalic anhydride
MTES	Methyltriethoxysilane
MTMS	Methyltrimethoxysilane
MTMOS	Methyltrimethyl orthosilane
MPs	Microparticles
NPs	Nanoparticles
D4	Octamethylcyclotetrasiloxane (D4)
PCT	Polycondensation of tetrasiloxanetetraols (PCT)
PCMSQ	Poly(chloropropyl-methyl)silsesquioxanes
PMMA	Poly(methyl methacrylate)
PCT	Polycondensation of cyclic tetrasiloxanetetraols
POSS	Polyhedral oligomeric silsesquioxanes
PMSQ	Polymethyl silsesquioxane
PSQ	Polysilsesquioxane
PS	Polystyrene (PS)
PU	Polyurethane (PU)
SPI	Soluble polyimide (SPI)
SCP	Step-wise coupling polymerization
SDB	Styrene-divinylbenzene
TBHP	*tert*-Butylhydroperoxide
MTOS	Tetramethyl orthosilane
TSQ	Thermally treated silsesquioxanes
TTACl	Trimethyl[3(triethoxysilyl)propyl]ammonium chloride
TPE-PDT	Two-photon excited photodynamic therapy
WCA	Water contact angle

Acknowledgements

Financial support from the National Key R&D Program of China (No. 2017YFE0116000) and National Natural Science Foundation of China (No. 21875131) are gratefully acknowledged.

References

1 S. Li, J. Huang, Z. Chen, G. Chen and Y. Lai, A review on special wettability textiles: theoretical models, fabrication technologies and multifunctional applications, *J. Mater. Chem. A*, 2017, **5**(1), 31–55.

2 N. Liu, Q. Du, G. Yin, P. Liu, L. Li, H. Xie, *et al.*, Extremely low trap-state energy level perovskite solar cells passivated using NH 2 -POSS with improved efficiency and stability, *J. Mater. Chem. A*, 2018, **6**(16), 6806–6814.

3 M. D'Arienzo, S. Diré, M. Redaelli, E. Borovin, E. Callone, B. Di Credico, *et al.*, Unveiling the hybrid interface in polymer nanocomposites enclosing silsesquioxanes with tunable molecular structure: Spectroscopic, thermal and mechanical properties, *J. Colloid Interface Sci.*, 2018, **512**, 609–617.

4 J. G. Croissant, Y. Fatieiev and N. M. Khashab, Degradability and Clearance of Silicon, Organosilica, Silsesquioxane, Silica Mixed Oxide, and Mesoporous Silica Nanoparticles, *Adv. Mater.*, 2017, **29**, 1604634.

5 R. Mazzaro, F. Romano and P. Ceroni, Long-lived luminescence of silicon nanocrystals: From principles to applications, *Phys. Chem. Chem. Phys.*, 2017, **19**, 26507–26526.

6 H. Hodaei, A. U. Hassan, S. Wittek, H. Garcia-Gracia, R. El-Ganainy, D. N. Christodoulides, *et al.*, Enhanced sensitivity at higher-order exceptional points, *Nature*, 2017, **548**(7666), 187–191.

7 Y. Chen and J. Shi, Chemistry of Mesoporous Organosilica in Nanotechnology: Molecularly Organic-Inorganic Hybridization into Frameworks, *Adv. Mater.*, 2016, **28**, 3235–3272.

8 J. G. Croissant, Y. Fatieiev, A. Almalik and N. M. Khashab, Mesoporous Silica and Organosilica Nanoparticles: Physical Chemistry, Biosafety, Delivery Strategies, and Biomedical Applications, *Adv. Healthcare Mater.*, 2018, **7**, 1700831.

9 H. Chi, M. Wang, Y. Xiao, F. Wang and K. S. Joshy, Self-assembly and applications of amphiphilic hybrid poss copolymers, *Molecules*, 2018, **23**, 23102481.
10 X. Qiao, R. Chen, H. Yan and S. Shen, Polyhedral oligomeric silsesquioxane-based hybrid monolithic columns: Recent advances in their preparation and their applications in capillary liquid chromatography, *TrAC, Trends Anal. Chem.*, 2017, **97**, 50–64.
11 Y. Li, X. H. Dong, Y. Zou, Z. Wang, K. Yue, M. Huang, *et al.*, Polyhedral oligomeric silsesquioxane meets "click" chemistry: Rational design and facile preparation of functional hybrid materials, *Polymer*, 2017, **125**, 303–329.
12 J. Su, L. Yang and Q. Wang, Dual polyhedral oligomeric silsesquioxanes polymerization approach to mutually-mediated separation mechanisms of hybrid monolithic stationary and mobile phases towards small molecules, *J. Chromatogr. A*, 2018, **1533**, 136–142.
13 N. Liu, J. Yu, Y. Meng and Y. Liu, Hyperbranched polysiloxanes based on polyhedral oligomeric silsesquioxane cages with ultra-high molecularweight and structural tuneability, *Polymers*, 2018, **10**(5), 10050496.
14 X. Wang, Y. Li, Y. Qian, H. Qi, J. Li and J. Sun, Mechanically Robust Atomic Oxygen-Resistant Coatings Capable of Autonomously Healing Damage in Low Earth Orbit Space Environment, *Adv. Mater.*, 2018, **30**(36), 1803854.
15 S. J. Han, J. Tang, B. Kumar, A. Falk, D. Farmer, G. Tulevski, *et al.*, High-speed logic integrated circuits with solution-processed self-assembled carbon nanotubes, *Nat. Nanotechnol.*, 2017, **12**(9), 861–865.
16 V. Flauraud, M. Mastrangeli, G. D. Bernasconi, J. Butet, D. T. L. Alexander, E. Shahrabi, *et al.*, Nanoscale topographical control of capillary assembly of nanoparticles, *Nat. Nanotechnol.*, 2017, **12**(1), 73–80.
17 Z. Li, X. Liu, X. J. Loh, X. Fan, L. Jiang and Y.-L. Wu, Biodegradable polyester unimolecular systems as emerging materials for therapeutic applications, *J. Mater. Chem. B*, 2018, **6**(35), 5488–5498.
18 F. Dong, L. Lu and C. S. Ha, Silsesquioxane-Containing Hybrid Nanomaterials: Fascinating Platforms for Advanced Applications, *Macromol. Chem. Phys.*, 2019, **220**, 1800324.
19 V. Vijayakumar and S. Y. Nam, Recent advancements in applications of alkaline anion exchange membranes for polymer electrolyte fuel cells, *J. Ind. Eng. Chem.*, 2019, **70**, 70–86.
20 X. Chen and L. F. Dumée, Polyhedral Oligomeric Silsesquioxane (POSS) Nano-Composite Separation Membranes – A Review, *Adv. Eng. Mater.*, 2018, 1800667.
21 E. Dornsiepen, E. Geringer, N. Rinn and S. Dehnen, Coordination chemistry of organometallic or inorganic binary group 14/16 units towards d-block and f-block metal atoms, *Coord. Chem. Rev.*, 2019, **380**, 136–169.
22 K. B. Lynch, J. Ren, M. A. Beckner, C. He and S. Liu, Monolith columns for liquid chromatographic separations of intact proteins: A review of recent advances and applications, *Anal. Chim. Acta*, 2019, **1046**, 48–68.
23 F. Yang, B. Yao, C. Li, G. Sun and X. Ma, Oil dispersible polymethylsilsesquioxane (PMSQ) microspheres improve the flow behavior of waxy crude oil through spacial hindrance effect, *Fuel*, 2017, **199**, 4–13.
24 J. Graffion, D. Dems, M. Demirelli, T. Coradin, N. Delsuc and C. Aimé, An All-in-One Molecule for the One-Step Synthesis of Functional Hybrid Silica Particles with Tunable Sizes, *Eur. J. Inorg. Chem.*, 2017, **2017**(43), 5047–5051.
25 S. Sakamoto, K. Fujino, A. Shimojima and K. Kuroda, Formation of Silica–Organic Hybrid Nanoparticles by Cross-linking of Ultra-small Silica Nanoparticles, *Chem. Lett.*, 2018, **47**(8), 1018–1021, DOI: 10.1246/cl.180374.
26 L. Zhang, P. Fu, B. Wang, M. Liu, Q. Zhao, X. Pang, *et al.*, Preparation of novel optically active polyamide@silica hybrid core-shell nanoparticles and application for enantioselective crystallization, *React. Funct. Polym.*, 2018, **131**, 326–332, available from: https://www.sciencedirect.com/science/article/pii/S1381514818305820.
27 H. S. Chae, S. J. Song and Y. H. Park, Preparation of spherical poly(methylsilsesquioxanes) beads and their properties, *Mol. Cryst. Liq. Cryst.*, 2008, **492**, 28–38.
28 S. C. Nunes, G. Toquer, M. A. Cardoso, A. Mayoral, R. A. S. Ferreira, L. D. Carlos, *et al.*, Structuring of Alkyl-Triazole Bridged Silsesquioxanes, *ChemistrySelect*, 2017, **2**(1), 432–442.
29 J. Yuan, W. Ma and J. Mo, Fabrication of highly monodisperse CeO2@poly(methyl silsesquioxane) microspheres and their application in UV-shielding films, *J. Appl. Polym. Sci.*, 2017, **134**(29), 45065.
30 Ł. John, M. Janeta and S. Szafert, Synthesis of cubic spherosilicates for self-assembled organic-inorganic biohybrids based on functionalized methacrylates, *New J. Chem.*, 2018, **42**(1), 39–47.
31 J. G. Croissant, X. Cattoën, J.-O. Durand, M. Wong Chi Man and N. M. Khashab, Organosilica hybrid nanomaterials with a high organic content: syntheses and applications of silsesquioxanes, *Nanoscale*, 2016, **8**(48), 19945–19972.
32 D. J. Krug and R. M. Laine, Durable and Hydrophobic Organic-Inorganic Hybrid Coatings via Fluoride Rearrangement of Phenyl T12Silsesquioxane and Siloxanes, *ACS Appl. Mater. Interfaces*, 2017, **9**(9), 8378–8383.
33 R. Misra, B. X. Fu and S. E. Morgan, Surface energetics, dispersion, and nanotribomechanical behavior of POSS/PP hybrid nanocomposites, *J. Polym. Sci., Part B: Polym. Phys.*, 2007, **45**(17), 2441–2455.
34 T. Hirohara, T. Kai, J. Ohshita and Y. Kaneko, Preparation of protic ionic liquids containing cyclic oligosiloxane frameworks, *RSC Adv.*, 2017, **7**(17), 10575–10582.
35 M. M. Levitsky, A. N. Bilyachenko and G. B. Shul'pin, Oxidation of C-H compounds with peroxides catalyzed by polynuclear transition metal complexes in Si- or Ge-sesquioxane frameworks: A review, *J. Organomet. Chem.*, 2017, **849–850**, 201–218.

36 H. Zhou, H. Wang, H. Niu and T. Lin, Recent Progress in Durable and Self-Healing Super-Nonwettable Fabrics, *Adv. Mater. Interfaces*, 2018, **5**, 1800461.

37 H. Gao, P. Sun, Y. Zhang, X. Zeng, D. Wang, Y. Zhang, *et al.*, A two-step hydrophobic fabrication of melamine sponge for oil absorption and oil/water separation, *Surf. Coat. Technol.*, 2018, **339**, 147–154.

38 Y. F. Lin and S. H. Hsu, Solvent-resistant CTAB-modified polymethylsilsesquioxane aerogels for organic solvent and oil adsorption, *J. Colloid Interface Sci.*, 2017, **485**, 152–158.

39 S. H. Tolbert, P. D. McFadden and D. A. Loy, New Hybrid Organic/Inorganic Polysilsesquioxane–Silica Particles as Sunscreens, *ACS Appl. Mater. Interfaces*, 2016, **8**(5), 3160–3174, available from: http://pubs.acs.org/doi/10.1021/acsami.5b10472.

40 Z. Wang, Z. Qian, Y. Cao, X. Zhang, R. Tai, H. Dong, *et al.*, Facile preparation of bridged silsesquioxane microspheres with interconnected multi-cavities and open holes, *RSC Adv.*, 2016, **6**(26), 21571–21576, DOI: 10.1039/c5ra22733j.

41 A. Bele, M. Dascalu, C. Tugui, M. Iacob, C. Racles, L. Sacarescu, *et al.*, Dielectric silicone elastomers filled with in situ generated polar silsesquioxanes: Preparation, characterization and evaluation of electromechanical performance, *Mater. Des.*, 2016, **106**, 454–462.

42 S. Sakka, History of the Sol–Gel Chemistry and Technology, in *Handbook of Sol–Gel Science and Technology*, 2016, pp. 1–27, available from: http://link.springer.com/10.1007/978-3-319-19454-7_87-1.

43 M. G. Mohamed and S. W. Kuo, Functional Silica and Carbon Nanocomposites Based on Polybenzoxazines, *Macromol. Chem. Phys.*, 2019, **220**, 1800306.

44 Z. Jin, H. Fan, B. G. Li and S. Zhu, Evaluation of Octyltetramethyldisiloxane-Containing Ethylene Copolymers as Composite Lubricant for High-Density Polyethylene, *Macromol. Mater. Eng.*, 2016, **301**(12), 1494–1502.

45 F. U. Khan, L. Cheng, M. Haroon, T. Aziz and H. Fan, Modified silicone oil types, mechanical properties and applications, *Polym. Bull.*, 2018, 2129–2145.

46 H. Fan, C. Bittencourt, Z. Ma, X. Zhang, P. Dubois and J. Wan, A novel polyhedral oligomeric silsesquioxane-modified layered double hydroxide: preparation, characterization and properties, *Beilstein J. Nanotechnol.*, 2018, **9**, 3053–3068.

47 B. Yao, X. Zhang, F. Yang, C. Li, G. Sun, G. Zhang, *et al.*, Morphology-controlled synthesis of polymethylsilsesquioxane (PMSQ) microsphere and its applications in enhancing the thermal properties and flow improving ability of ethylene-vinyl acetate copolymer, *Powder Technol.*, 2018, **329**, 137–148.

48 Z. Jin, H. Fan, B. G. Li and S. Zhu, Synthesis of a novel type of octyltetramethyldisiloxane-containing olefinic macromonomer and its copolymerization with ethylene, *Polymer*, 2016, **83**, 20–26, available from: http://dx.doi.org/10.1016/j.polymer.2015.11.058.

49 S. G. Kwon and T. Hyeon, Formation mechanisms of uniform nanocrystals via hot-injection and heat-up methods, *Small*, 2011, **7**, 2685–2702.

50 W. Zhang, X. Li and R. Yang, Flame retardancy mechanisms of phosphorus-containing polyhedral oligomeric silsesquioxane (DOPO-POSS) in polycarbonate/acrylonitrile-butadiene-styrene blends, *Polym. Adv. Technol.*, 2012 Mar, **23**(3), 588–595.

51 A. Fina, O. Monticelli and G. Camino, POSS-based hybrids by melt/reactive blending, *J. Mater. Chem.*, 2010, **20**(42), 9297, available from: http://xlink.rsc.org/?DOI=c0jm00480d.

52 A. Harada, S. Koge, J. Ohshita and Y. Kaneko, Preparation of a thermally stable room temperature ionic liquid containing cage-like oligosilsesquioxane with two types of side-chain groups, *Bull. Chem. Soc. Jpn.*, 2016, **89**(9), 1129–1135.

53 H. Bagheri, G. Soofi, H. Javanmardi and M. Karimi, A 3D nanoscale polyhedral oligomeric silsesquioxanes network for microextraction of polycyclic aromatic hydrocarbons, *Microchim. Acta*, 2018, **185**(9), 418, available from: https://doi.org/10.1007/s00604-018-2950-z.

54 L. Huo, X. Wu, C. Tian and J. Gao, Thermal, Mechanical, and Electrical Properties of Alkyd-Epoxy Resin Nanocomposites Modified with 3-Glycidyloxypropyl-POSS, *Polym.-Plast. Technol. Eng.*, 2018, **57**(5), 371–379, available from: https://doi.org/10.1080/03602559.2016.1185619.

55 A. Kowalewska, Self-Assembling Polyhedral Silsesquioxanes - Structure and Properties, *Curr. Org. Chem.*, 2017, **21**(14), 1243–1264, available from: http://www.eurekaselect.com/node/150597/article.

56 A. N. Bilyachenko, A. N. Kulakova, M. M. Levitsky, A. A. Petrov, A. A. Korlyukov, L. S. Shul'pina, *et al.*, Unusual Tri-, Hexa-, and Nonanuclear Cu(II) Cage Methylsilsesquioxanes: Synthesis, Structures, and Catalytic Activity in Oxidations with Peroxides, *Inorg. Chem.*, 2017, **56**(7), 4093–4103.

57 P. A. Wheeler, B. X. Fu, J. D. Lichtenhan, W. Jia and L. J. Mathias, Incorporation of metallic POSS, POSS copolymers, and new functionalized POSS compounds into commercial dental resins, *J. Appl. Polym. Sci.*, 2006, **102**(3), 2856–2862.

58 Z. Li and R. Yang, Synthesis, characterization, and properties of a polyhedral oligomeric octadiphenylsulfonylsilsesquioxane, *J. Appl. Polym. Sci.*, 2014, **131**(20), 40892, available from: http://doi.wiley.com/10.1002/app.40892.

59 Z. Li, D. Li and R. Yang, Synthesis, characterization, and properties of a novel polyhedral oligomeric octamethyldiphenylsulfonylsilsesquioxane, *J. Mater. Sci.*, 2015, **50**(2), 697–703, available from: http://link.springer.com/10.1007/s10853-014-8629-x.

60 J. Croissant, M. Maynadier, O. Mongin, V. Hugues, M. Blanchard-Desce, A. Chaix, *et al.*, Enhanced two-photon fluorescence imaging and therapy of cancer cells via Gold@Bridged silsesquioxane nanoparticles, *Small*, 2015, **11**(3), 295–299.

61 S. Dirè, V. Tagliazucca, E. Callone and A. Quaranta, Effect of functional groups on condensation and properties of sol-gel silica nanoparticles prepared by direct synthesis from organoalkoxysilanes, *Mater. Chem. Phys.*, 2011, **126**(3), 909–917.

62 S. L. Greasley, S. J. Page, S. Sirovica, S. Chen, R. A. Martin, A. Riveiro, *et al.*, Controlling particle size in the Stöber process and incorporation of calcium, *J. Colloid Interface Sci.*, 2016, **469**, 213–223.

63 G. Hayase, K. Kugimiya, M. Ogawa, Y. Kodera, K. Kanamori and K. Nakanishi, The thermal conductivity of polymethylsilsesquioxane aerogels and xerogels with varied pore sizes for practical application as thermal superinsulators, *J. Mater. Chem. A*, 2014, **2**(18), 6525–6531.

64 G. M. Luz and J. F. Mano, Preparation and characterization of bioactive glass nanoparticles prepared by sol-gel for biomedical applications, *Nanotechnology*, 2011, **22**(49), 494014.

65 F. Devreux, J. P. Boilot, F. Chaput and A. Lecomte, Sol-gel condensation of rapidly hydrolyzed silicon alkoxides: A joint Si29 NMR and small-angle x-ray scattering study, *Phys. Rev. A: At., Mol., Opt. Phys.*, 1990, **41**(12), 6901–6909.

66 V. P. Swapna, S. P. Thomas, T. Jose, G. Moni, S. C. George, S. Thomas, *et al.*, Mechanical properties and pervaporation separation performance of CTAB-modified cage-structured POSS-incorporated PVA membrane, *J. Mater. Sci.*, 2019, **54**(11), 8319–8331.

67 C. Mauriello-Jimenez, M. Henry, D. Aggad, L. Raehm, X. Cattoën, M. Wong Chi Man, *et al.*, Porphyrin- or phthalocyanine-bridged silsesquioxane nanoparticles for two-photon photodynamic therapy or photoacoustic imaging, *Nanoscale*, 2017, **9**(43), 16622–16626.

68 D. Kim, K. Shin, S. G. Kwon and T. Hyeon, Synthesis and Biomedical Applications of Multifunctional Nanoparticles, *Adv. Mater.*, 2018, **30**, 1802309.

69 X. Du, F. Kleitz, X. Li, H. Huang, X. Zhang and S. Z. Qiao, Disulfide-Bridged Organosilica Frameworks: Designed, Synthesis, Redox-Triggered Biodegradation, and Nanobiomedical Applications, *Adv. Funct. Mater.*, 2018, **28**(26), 1707325.

70 M. Ge and H. Liu, A silsesquioxane-based thiophene-bridged hybrid nanoporous network as a highly efficient adsorbent for wastewater treatment, *J. Mater. Chem. A*, 2016, **4**(42), 16714–16722.

71 D. V. Quang, A. Dindi, K. Al-Ali and M. R. M. Abu-Zahra, Template-free amine-bridged silsesquioxane with dangling amino groups and its CO2 adsorption performance, *J. Mater. Chem. A*, 2018, **6**(46), 23690–23702.

72 J. Kaźmierczak and G. Hreczycho, Catalytic Approach to Germanium-Functionalized Silsesquioxanes and Germasilsesquioxanes, *Organometallics*, 2017, **36**(19), 3854–3859.

73 N. Katsuta, M. Yoshimatsu, K. Komori, T. Natsuaki, K. Suwa, K. Sakai, *et al.*, Necklace-shaped dimethylsiloxane polymers bearing polyhedral oligomeric silsesquioxane cages with alternating length chains, *Polymer*, 2017, **127**, 8–14.

74 A. Baatti, F. Erchiqui, P. Bébin, F. Godard and D. Bussières, A two-step Sol-Gel method to synthesize a ladder polymethylsilsesquioxane nanoparticles, *Adv. Powder Technol.*, 2017, **28**(3), 1038–1046.

75 F. Brunet and B. Cabane, Populations of oligomers in sol-gel condensation, *J. Non-Cryst. Solids*, 1993, **163**(3), 211–225.

76 W. E. Wallace, C. M. Guttman and J. M. Antonucci, Molecular structure of silsesquioxanes determined by matrix-assisted laser desorption/ionization time-of-flight mass spectrometry, *J. Am. Soc. Mass Spectrom.*, 1999, **10**(3), 224–230, available from: https://www.sciencedirect.com/science/article/pii/S1044030598001470.

77 L. Matějka, O. Dukh, D. Hlavatá, B. Meissner and J. Brus, Cyclization and self-organization in polymerization of trialkoxysilanes, *Macromolecules*, 2001, **34**(20), 6904–6914.

78 J. K. Crandall and C. Morel-Fourrier, Siloxanes from the hydrolysis of isopropyltrimethoxysilane, *J. Organomet. Chem.*, 1995, **489**(1–2), 5–13.

79 A. Harada, K. Shikinaka, J. Ohshita and Y. Kaneko, Preparation of a one-dimensional soluble polysilsesquioxane containing phosphonic acid side-chain groups and its thermal and proton-conduction properties, *Polymer*, 2017, **121**, 228–233.

80 S. O. Hwang, A. S. Lee, J. Y. Lee, S. H. Park, K. I. Jung, H. W. Jung, et al. Mechanical properties of ladder-like polysilsesquioxane-based hard coating films containing different organic functional groups, *Prog. Org. Coat.*, 2018, **121**, 105–111.

81 Y. Y. Jo, A. S. Lee, K. Y. Baek, H. Lee and S. S. Hwang, Thermally reversible self-healing polysilsesquioxane structure-property relationships based on Diels-Alder chemistry, *Polymer*, 2017, **108**, 58–65.

82 M. Nowacka, A. Kowalewska and T. Makowski, Structural studies on ladder phenylsilsesquioxane oligomers formed by polycondensation of cyclotetrasiloxanetetraols, *Polymer*, 2016, **87**, 81–89.

83 Y. H. Kim, G. M. Choi, J. G. Bae, Y. H. Kim and B. S. Bae, High-performance and simply-synthesized ladder-like structured methacrylate siloxane hybrid material for flexible hard coating, *Polymers*, 2018, **10**(4), 10040449.

84 A. N. Bilyachenko, A. I. Yalymov, A. A. Korlyukov, J. Long, J. Larionova, Y. Guari, *et al.*, Unusual penta- and hexanuclear Ni(II)-based silsesquioxane polynuclear complexes, *Dalton Trans.*, 2016, **45**(17), 7320–7327.

85 Z. Ren and S. Yan, Polysiloxanes for optoelectronic applications, *Prog. Mater. Sci.*, 2016, **83**, 383–416.

86 R. Kunthom, P. Piyanuch, N. Wanichacheva and V. Ervithayasuporn, Cage-like silsesequioxanes bearing rhodamines as fluorescence Hg2+ sensors, *J. Photochem. Photobiol., A*, 2018, **356**, 248–255.

87 C. Lei, Z. Hu, Y. Zhang, H. Yang, J. Li and S. Hu, Tailoring structural and physical properties of polymethylsilsesquioxane aerogels by adjusting NH3·H2O concentration, *Microporous Mesoporous Mater.*, 2018, **258**, 236–243.

88 J. Kaźmierczak, K. Kuciński and G. Hreczycho, Highly Efficient Catalytic Route for the Synthesis of Functionalized Silsesquioxanes, *Inorg. Chem.*, 2017, **56**(15), 9337–9342.

89 J. Sun and L. Deng, Cobalt Complex-Catalyzed Hydrosilylation of Alkenes and Alkynes, *ACS Catal.*, 2016, **6**(1), 290–300, available from: http://pubs.acs.org/doi/10.1021/acscatal.5b02308.

90 H. K. Carroll, F. G. L. Parlane, N. Reich, B. J. Jelier and C. D. Montgomery. Phosphoramidite complexes of Pd(II), Pt(II) and Rh(I): An effective hydrosilylation catalyst of 1-hexyne and 1-octene, *Inorg. Chim. Acta,* 2017, **465**, 78–83, available from: https://www.sciencedirect.com/science/article/pii/S0020169317301937.

91 A. Franczyk, K. Stefanowska, M. Dutkiewicz, D. Frąckowiak and B. Marciniec, A highly selective synthesis of new alkenylsilsesquioxanes by hydrosilylation of alkynes, *Dalton Trans.*, 2017, **46**(1), 158–164.

92 K. Mituła, M. Dutkiewicz, B. Dudziec, B. Marciniec and K. Czaja, A library of monoalkenylsilsesquioxanes as potential comonomers for synthesis of hybrid materials, *J. Therm. Anal. Calorim.*, 2018, **132**(3), 1545–1555.

93 J. Kaźmierczak and G. Hreczycho, Nafion as effective and selective heterogeneous catalytic system in O-metalation of silanols and POSS silanols, *J. Catal.*, 2018, **367**, 95–103.

94 D. Chen, W. Sun, C. Qian, L. M. Reyes, A. P. Y. Wong, Y. Dong, *et al.*, Porous NIR Photoluminescent Silicon Nanocrystals-POSS Composites, *Adv. Funct. Mater.*, 2016, **26**(28), 5102–5110.

95 X. You, H. Wu, Y. Su, J. Yuan, R. Zhang, Q. Yu, *et al.*, Precise nanopore tuning for a high-throughput desalination membrane via co-deposition of dopamine and multifunctional POSS, *J. Mater. Chem. A*, 2018, **6**(27), 13191–13202.

96 R. Al-Attabi, L. F. Dumée, L. Kong, J. A. Schütz and Y. Morsi, High Efficiency Poly(acrylonitrile) Electrospun Nanofiber Membranes for Airborne Nanomaterials Filtration, *Adv. Eng. Mater.*, 2018, **20**(1), 1700572.

97 X. Chen, Z. Chen, L. F. Dumée, L. A. O'Dell, J. du Plessis, R. d'Agostino, *et al.*, Grafting of N-moieties onto octa-methyl polyhedral oligomeric silsesquioxane microstructures by sequential continuous wave and pulsed plasma, *Plasma Processes Polym.*, 2017, **14**(10), 1600244.

98 Y. Yoon and T. S. Lee, Preparation of liquid marbles using an azobenzene-based metal-organic framework particles, *Mol. Cryst. Liq. Cryst.*, 2018, **660**(1), 90–97.

99 Y. Y. Jo, A. S. Lee, K. Y. Baek, H. Lee and S. S. Hwang, Multi-crosslinkable self-healing polysilsesquioxanes for the smart recovery of anti-scratch properties, *Polymer*, 2017, **124**, 78–87.

100 L. Xin, Q. Yin, Z. Xin and Z. Zhang, Powerful adsorption of silver(I) onto thiol-functionalized polysilsesquioxane microspheres, *Chem. Eng. Sci.*, 2010, **65**(24), 6471–6477.

101 M. Szołyga, M. Dutkiewicz and B. Marciniec, Polyurethane composites based on silsesquioxane derivatives of different structures, *J. Therm. Anal. Calorim.*, 2018, **132**(3), 1693–1706.

102 K. I. Jung, S. O. Hwang, N. H. Kim, D. G. Lee, J. H. Lee and H. W. Jung, Effect of methacryloxypropyl and phenyl functional groups on crosslinking and rheological and mechanical properties of ladder-like polysilsesquioxane hard coatings, *Prog. Org. Coat.*, 2018, **124**, 129–136.

103 Z. Ma, C. Li, H. Fan, J. Wan, Y. Luo and B. G. Li, Polyhydroxyurethanes (PHUs) Derived from Diphenolic Acid and Carbon Dioxide and Their Application in Solvent- and Water-Borne PHU Coatings, *Ind. Eng. Chem. Res.*, 2017, **56**(47), 14089–14100.

104 Y. Kaneko, H. Imamura, T. Sugioka and Y. Sumida, Preparation and thermal properties of soluble polysilsesquioxanes containing hydrophobic side-chain groups and their hybridization with organic polymers, *Polymer*, 2016, **92**, 250–255.

105 M. Mirzaee and M. Faghani, Preparation and characterization of micro-spherical poly-organo-silsesquioxane immobilized ligand systems to support MoO2(acac)2and investigation of their catalytic properties in epoxidation of alkenes, *J. Sol-Gel Sci. Technol.*, 2018, **85**(3), 664–676.

106 C. Li, H. Fan, T. Aziz, C. Bittencourt, L. Wu, D. Y. Wang, et al. Biobased Epoxy Resin with Low Electrical Permissivity and Flame Retardancy: From Environmental Friendly High-Throughput Synthesis to Properties, *ACS Sustainable Chem. Eng.*, 2018, **6**(7), 8856–8867.

107 E. Husamelden and H. Fan, Fluorinated functionalization of graphene oxide and its role as a reinforcement in epoxy composites, *J. Polym. Res.*, 2019, **26**(2), 42.

108 M. Walczak, K. Stefanowska, A. Franczyk, J. Walkowiak, A. Wawrzyńczak and B. Marciniec, Hydrosilylation of alkenes and alkynes with silsesquioxane (HSiMe2O)(i-Bu) 7Si8O12catalyzed by Pt supported on a styrene-divinylbenzene copolymer, *J. Catal.*, 2018, **367**, 1–6.

109 E. Roduner, Size matters: Why nanomaterials are different, *Chem. Soc. Rev.*, 2006, **35**, 583–592.

110 J. G. Croissant, X. Cattoën, J. O. Durand, M. Wong Chi Man and N. M. Khashab, Organosilica hybrid nanomaterials with a high organic content: syntheses and applications of silsesquioxanes, *Nanoscale*, 2016, **8**(48), 19945–19972.

111 S. Mohapatra, T. Chaiprasert, R. Sodkhomkhum, R. Kunthom, S. Hanprasit, P. Sangtrirutnugul, *et al.*, Solid–state Synthesis of Polyhedral Oligomeric Silsesquioxane-Supported N-Heterocyclic Carbenes/Imidazolium salts on Palladium Nanoparticles: Highly Active and Recyclable Catalyst, *ChemistrySelect*, 2016, **1**(16), 5353–5357.

112 A. R. Hamilton, N. R. Sottos and S. R. White, Self-Healing of Internal Damage in Synthetic Vascular Materials, *Adv. Mater.*, 2010, **22**(45), 5159–5163, available from: http://doi.wiley.com/10.1002/adma.201002561.

113 Z. Xu, Y. Zhao, X. Wang and T. Lin, A thermally healable polyhedral oligomeric silsesquioxane (POSS) nanocomposite based on Diels-Alder chemistry, *Chem. Commun.*, 2013, **49**(60), 6755–6757.

114 S. Fahad, H. Yu, L. Wang, Zain-ul-Abdin, M. Haroon, R. S. Ullah, *et al.*, Recent progress in the synthesis of silver nanowires and their role as conducting materials, *J. Mater. Sci.*, 2019, **54**, 997–1035.

115 A. Nazir, H. Yu, L. Wang, M. Haroon, R. S. Ullah, S. Fahad, *et al.*, Recent progress in the modification of carbon materials and their application in composites for electromagnetic interference shielding, *J. Mater. Sci.*, 2018, **53**(12), 8699–8719.

116 M. Haroon, L. Wang, H. Yu, N. M. Abbasi, Zain-Ul-Abdin, M. Saleem, *et al.*, Chemical modification of starch and its application as an adsorbent material, *RSC Adv.*, 2016, **6**, 78264–78285.

117 M. Mirzaee, B. Bahramian and A. Amoli, Schiff base-functionalized boehmite nanoparticle-supported molybdenum and vanadium complexes: Efficient catalysts for the epoxidation of alkenes, *Appl. Organomet. Chem.*, 2015, **29**(9), 593–600.

118 W. Fan, D. Shi and B. Feng, Immobilizing of oxo-molybdenum complex on cross-linked copolymer and its catalytic activity for epoxidation reactions, *Catal. Commun.*, 2016, **74**, 1–4.

119 M. Mohammadikish, M. Masteri-Farahani and S. Mahdavi, Immobilized molybdenum–thiosemicarbazide Schiff base complex on the surface of magnetite nanoparticles as a new nanocatalyst for the epoxidation of olefins, *J. Magn. Magn. Mater.*, 2014, **354**, 317–323, available from: http://www.sciencedirect.com/science/article/pii/S0304885313008056.

120 Y. Yang, S. Hao, Y. Zhang and Q. Kan, Oxovanadium(IV) and dioxomolybdenum(VI) salen complexes tethered onto amino-functionalized SBA-15 for the epoxidation of cyclooctene, *Solid State Sci.*, 2011, **13**(11), 1938–1942, available from: http://www.sciencedirect.com/science/article/pii/S129325581100272X.

121 M. Moghadam, S. Tangestaninejad, V. Mirkhani, I. Mohammadpoor-Baltork and N. S. Mirbagheri, Molybdenum hexacarbonyl supported on functionalized multi-wall carbon nanotubes: Efficient and highly reusable catalysts for epoxidation of alkenes with tert-butyl hydroperoxide, *J. Organomet. Chem.*, 2010, **695**(17), 2014–2021, available from: http://www.sciencedirect.com/science/article/pii/S0022328X1000255X.

122 H. Maleki, L. Whitmore and N. Hüsing, Novel multifunctional polymethylsilsesquioxane-silk fibroin aerogel hybrids for environmental and thermal insulation applications, *J. Mater. Chem. A*, 2018, **6**(26), 12598–12612.

123 M. I. Jamil, A. Ali, F. Haq, Q. Zhang, X. Zhan and F. Chen, Icephobic Strategies and Materials with Superwettability: Design Principles and Mechanism, *Langmuir*, 2018, **34**(50), 15425–15444, available from: http://pubs.acs.org/doi/10.1021/acs.langmuir.8b03276.

124 S. Y. Hsu, S. C. Lin, J. A. Wang, T. Y. Cheng, C. W. Lin, Y. H. Chen, *et al.*, Preparation and characterization of silsesquioxane-graphene oxide modified soluble polyimide nanocomposites with excellent dispersibility and enhanced tensile properties, *Eur. Polym. J.*, 2019, **112**, 95–103.

